Design of a pneumatic thin wafer handler

Viehmann, Kelsey

Award date:
2018

Technische Universiteit
Eindhoven
University of Technology

Department of Mechanical Engineering
Section Control Systems Technology

VDL ETG T&D

Design of a pneumatic thin wafer handler

Master Thesis

CST 2018.058

Kelsey Viehmann

Supervisor:
dr. ir. P.C.J.N. Rosielle

Eindhoven, Tuesday 12th June, 2018

Contents

List of Figures

List of Tables

Chapter 1

Introduction

A wafer is a substrate often used in electronics manufacturing in the form of a circular disk with little height. Often silicon is used to form wafers since it is a relatively low cost material to fabricate through the Czochralski process[14]. Standard dimensions for a silicon wafer are a diameter of 200mm with a thickness of 725μm[1] or a diameter of 300mm with a thickness of 775μm[1]. Semiconductor devices such as integrated circuits(ICs) are produced on wafers through several micro fabrication steps[16][18][5], these ICs are the base for chips in phones, laptops, cameras, etc[16]. After these micro fabrication processes the wafer has a chip side (the manufactured side) and a back side[22]. A processed wafer, chipside visible, is shown in figure 1.1.

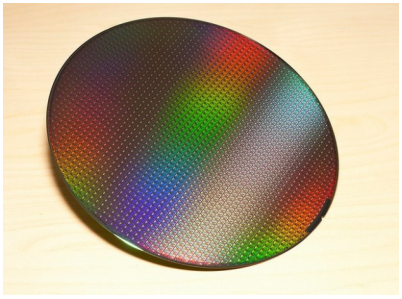

Figure 1.1: A standard wafer

In order to move wafers from one micro fabrication process step to the next they need to be handled by a handling robot[2][1]. During the microfabrication processes wafers are placed with the chipside on the wafer chuck[1]. The handling robot will pick the wafer, move the wafer and place it. The end-effector is the component of the wafer handler that touches and supports the wafer directly. The shape of the end effector for standard wafer handling is usually round, with the same diameter as the wafer[2], or fork shaped[2]. The force by which a standard wafer is secured on the end-effector is usually generated by either vacuum pads[2][22], electrostatic clamping[2][22] or by friction force[2][22].
After lithography, the wafers enter the back end process[16]. An overview of typical process steps in the back end process is shown in figure 1.2. During the back end process wafers are thinned and have to be handled in between each process step[22][16]. Process steps typical for the back end process are back grinding, (different types of) etching, polishing, bumping and inspection[5][18][7]. After these steps the wafer is transfered for the last time to the dicing station where the wafer will be cut into dies(small IC chips)[5][22][16].
The objective of this thesis is handling thin wafers between the process steps.

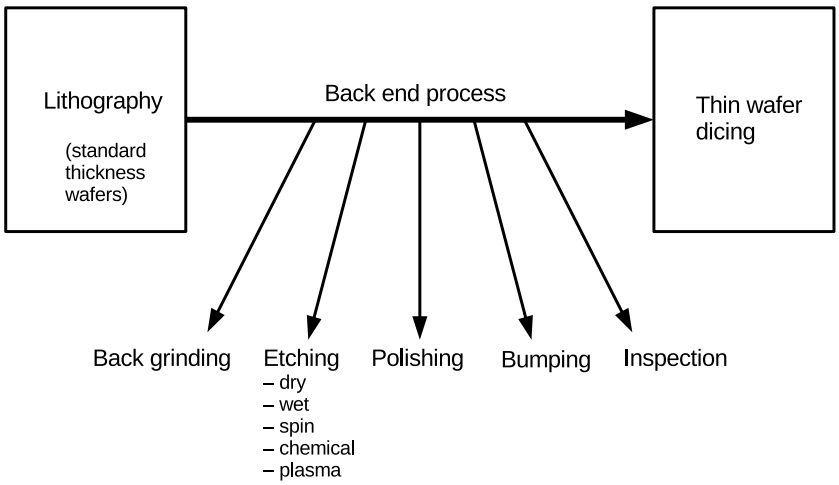

Figure 1.2: Overview of back end process and its process steps

Chapter 2

Investigation into thin wafer handling

This chapter provides background information on wafers, thin wafers, current handling solutions, issues with these solutions, the context for the thin wafer handler and the requirements for thin wafer handling.
In this chapter the surroundings of the handler will be discussed with the corresponding requirements and design volume as listed by VDL. Next a distinction between different categories of thin wafers will be made based on the handling methods available. Following the existing solutions will be reviewed with their respective challenges.

2.1 Context for the thin wafer handler

Noticeable with respect to the context is the fact that the thin wafer is processed in the back end process with the chip side down, facing the chuck. This implies handling the thin wafer on the top surface during the back end process.
The thin wafer handler will be situated in an atmospheric clean room environment[2]. The handler will pick up a wafer from a vacuum chuck of one process station and move the wafer to the vacuum chuck of the next process station where it will put the wafer down. The movement of the handler robot will be a rotation of 90 degrees around its central axis, displacing the wafer over a distance of 550mm. The handling enevelope therefore defined by VDL in the xy-plane is 600x600mm, as shown below in figure 2.1.
The thin wafer handler should also be able to pick up and place the wafer, which leads to a displacement in the z-direction executed by the handler robot. To accommodate for the arm of the handler and its displacement, the handling envelope in the yz/xz plane is 600x100 mm, also shown in 2.2. The height of the end-effector however, is limited by the design space, specified hereafter in this section.

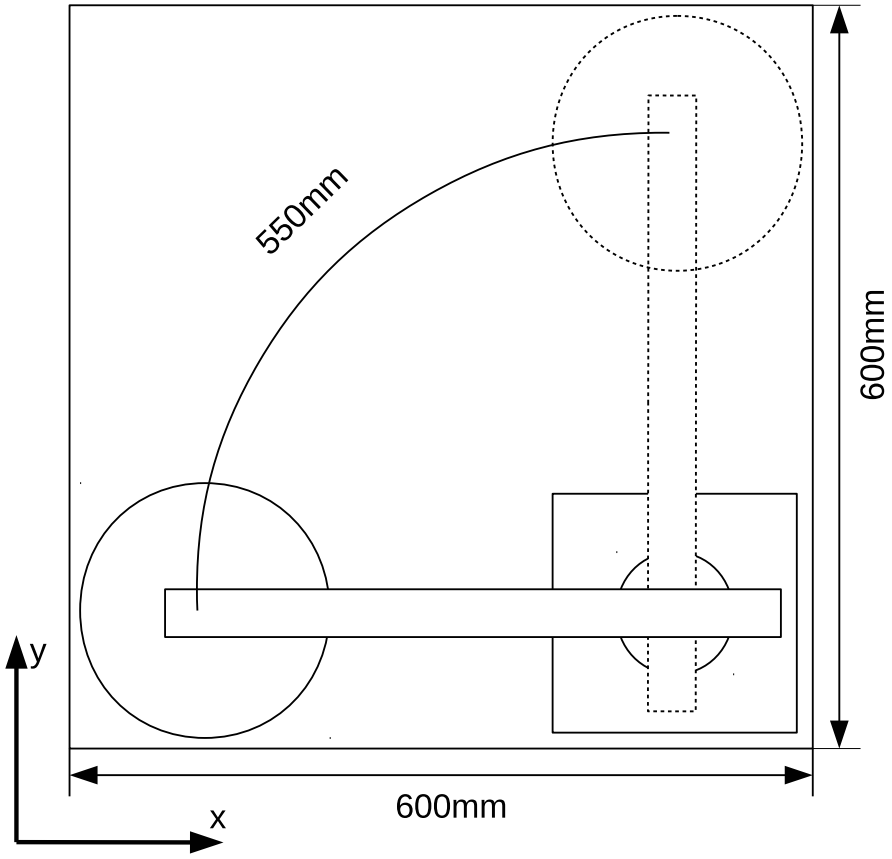

Figure 2.1: Top view of the handling enveloppe for a thin wafer

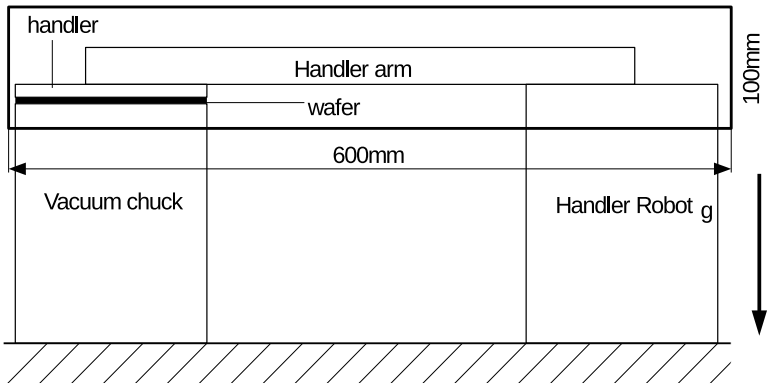

Figure 2.2: Side view of the handling envelope for a thin wafer

System requirements

Within VDL there was no prior experience with handling thin wafers, therefore the requirements as given do not yet contain any performance goals except handling time. Part of the assignment therefore was meant to translate the requirements below into the performance requirements.

- Clean room environment (cleanliness ISO 14644-1), with $T = 20 - 24C^{\circ}$ and a clean room relative humidity range of $30 - 60\%$[2].
- Not breaking the wafer during handling
- Not loosing the wafer during handling
- No excessive damage to the wafer during handling
- No substrate or carrier will have to be bonded to the wafer
- The requirement regarding the movement of the handler is that when placed on a robot it has to be able to pick, move and place the thin wafer in 10 seconds. The pick up of the thin wafer should be executed within 3.5 seconds. Next the movement in the xy-plane is also executed in 3.5 seconds. The placing of the wafer on the next process station has to be done within 3 seconds.

Design Space

The design space for the end-effector is limited further than the handling enveloppe. The design space is defined because the wafer handler needs to manoevre between process step features, for instance be able to move inside a load lock or inside a thin wafer FOUP(Front Opening Unified Pod, used to transfer wafers)[2]. This reduces the available height for the end-effector to 10mm.

Handler movements

The movements the handler undergos on top of the $z/\theta-$robot are determined below, from the starting point that the handling can take 10 seconds in total with 3.5s for the pick, 3.5s for xy-plane movement and 3s for place.
With a time of 3.5 seconds for the movement in the xy-plane of 550mm, the acceleration and velocity in x/y-direction are determined to be $a_{xy} = 0.81\frac{m}{s^2}$ and $v_{xy} = 0.94\frac{m}{s}$, with equations2.1 and 2.2.

$$a = \frac{2s}{t^2} \tag{2.1}$$

$$v = v_0 + at \tag{2.2}$$

The velocity profile for the movement in the xy-plane is shown below in figure 2.3.

This figure shows the movement profile for the robot on which the handler is placed, with a typical $\frac{1}{3}$, $\frac{1}{3}$, $\frac{1}{3}$ division of respectively the acceleration, constant speed and deceleration[2].

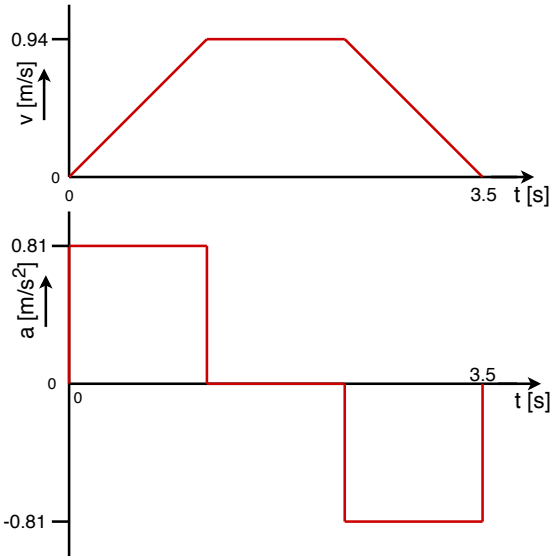

Figure 2.3: Velocity and acceleration profile for the x/y-direction movement

The movements in z-direction however can not take the full 3.5/3 seconds, as there is also time needed for the pneumatics to be activated and to settle.
The time allowed for the movement in z-direction for both pick and place is 2 seconds. In these 2 seconds the wafer is moved up or down 10mm. The movement profile for the z-direction is shown in figure 2.4. The maximum acceleration in z-direction resulting from the movement profile and equations2.1 and 2.2, is $a_z = 0.045\frac{m}{s^2}$. The velocity in z-direction is $v_z = 0.03\frac{m}{s}$.

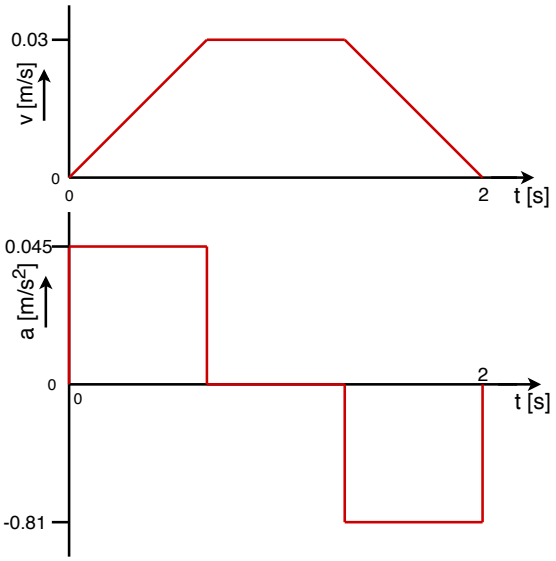

Figure 2.4: Velocity and acceleration profile for the z-direction movement

2.2 Categories of thin wafers

There are different categories of thin wafers by thickness, an overview of these categories is shown in 2.5. They are divided based on the commercialy available handling solutions. The categories can roughly be divided by thickness as follows: thickness$< 50\mu m$, thickness $50 - 100\mu m$ and a thickness of $t > 100\mu m$. One other thin wafer category is called TAIKO wafers[4], where the outside rim of the wafer remains of standard thickness and only the inside of the wafer is thinned to the desired thin wafer thickness.

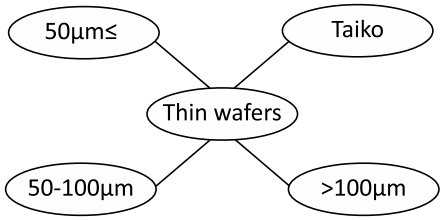

Figure 2.5: Overview of thin wafer categories

The devision by thickness as stated above is based handling solution properties per handling principle[22][16]. Wafers with a thickness smaller than $50\mu m$ are bonded to a carrier substrate temporarily to move through further process steps. They can not be handled by simply picking them up and placing them[16] because of their low stiffness. The wafer is bonded to the substrate carrier before the wafer is thinned below $50\mu m$[16]. Wafers with a thickness of $50\mu m$ have a stiffness approximately 8 times lower than the stiffness of a wafer of thickness $100\mu m$ [20]. This in combination with the higher number of available solutions for wafers of thickness $\geq 100\mu m$[8][10][12][15][11] defines the last two categories of thin wafers with $t \geq 100\mu m$ and $50 < t < 100\mu m$. Each category of thin wafers pointed out above has current handling solutions, which will be elaborated on in the next section.

2.3 Current handling solutions for thin wafers and their issues

There are roughly three different methods of attracting and clamping wafers with a thickness between $50-100\mu m$, namely pneumatic, electrostatic and mechanical clamping. [8][10][12][15][11][16].
Pneumatic handling is executed based on either blowing or sucking of air on/near the wafer[5]. Suction based devices usually have a series of small holes where a under pressure is created to clamp the wafer. Blowing devices, nicknamed Bernoulli grippers, force the air through a thin gap between the wafer and handler increasing the air's velocity and lowering its pressure to provide a clamping force[5].
Electrostatic handling is executed by alternating charges in the handler, creating an electrostatic force with respect to the wafer. As a result the wafer is clamped to the handler[5].
Mechanical solutions usually work by clamping the edge of the wafer by means of a spring force, or by placing the wafer on top of the end-effector and holding it by gravity induced friction [15][10][22]. A more elaborate explanation of the principles as well as an overview of the handling principles corresponding with the thin wafer categories is shown in Appendix A.
Thinning of the wafers has several side effects leading to challenges with their handling. One noticeable effect of the back end process on the thinning of the wafer is shown in figure 2.6. A standard wafer has rounded edges, by thinning this wafer the edges will become razor sharp and fragile[22]. Another effect of the thinning is that crack initiation starts in the wafer[16] and micro cracks form. These cracks are prone to fracture the wafer when a load is applied. Thin wafers have

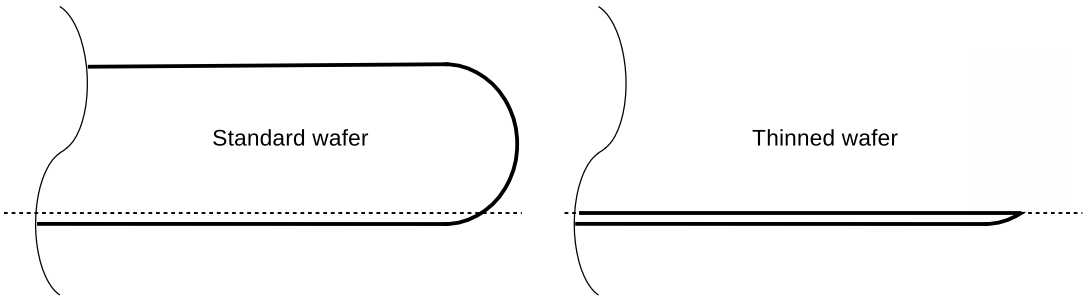

Figure 2.6: Illustration of the effect of the thinning process on a wafer with thickness of $725\mu m$ and $50\mu m$ respectively

the property to adhere to a flat, because of the vanderwaals forces. They are impossible to pick up from this flat without wrinkling the wafer, or sliding it over the flat. The properties of a thin wafer require for a handling method that exerts the minimal amount of force necessary to clamp the wafer while simultaneously having minimal contact area between the wafer and the handler, distributed evenly on the wafer area. This combination is not yet used in commercially available thin wafer handling solutions[8][10][12][15][11][16], discovered in the research for this thesis.
By providing a solution that combines these two properties this thesis is providing a possible method to handle wafer of $50\mu m$ without the need of a carrier.

2.4 Performance requirements for thin wafer handling

The concept design in this thesis should meet the following requirements to be able to handle thin wafers with a diameter of 200mm and a thickness of $50 - 70\mu m$.

- Clean room environment (cleanliness ISO 14644-1), with $T = 20 - 24C^{\circ}$ and a clean room relative humidity range of $30 - 60\%$[2].
- Acceleration in the x/y-direction of $a_{xy} = 0.81\frac{m}{s^2}$
- Velocity in the x/y-direction of $v_{xy} = 0.94\frac{m}{s}$
- Acceleration in the z-direction of $a_z = 0.045\frac{m}{s^2}$
- Velocity in the z-direction of $v_z = 0.03\frac{m}{s}$
- Transfer wafer from handler to chuck in X seconds
- Minimal contact area
- Minimal clamping force distributed over entire wafer surface
- No high stress concentrations on the wafer
- No contact on the edge

These requirements in combination with the thin wafer behaviour lead to the conclusion that the wafer needs to be picked up and held with not more force than absolutely necessary. This force should be distributed over the surface area of the wafer, with little contact surface area, to prevent damage to the wafer resulting from force concentrations.

Chapter 3

Thin wafer handler design concept

3.1 Design concept overview

In figure 3.1 the design concept for the pneumatic handling of $50 - 70\mu m$ thin wafers is shown. The design uses a slight under pressure to provide the force required to pick up the wafer and hold it. A pneumatic solution is chosen based on the desire to distributed the force on the surface area of the wafer, with little contact surface area, to prevent damage to the wafer resulting from force concentrations.

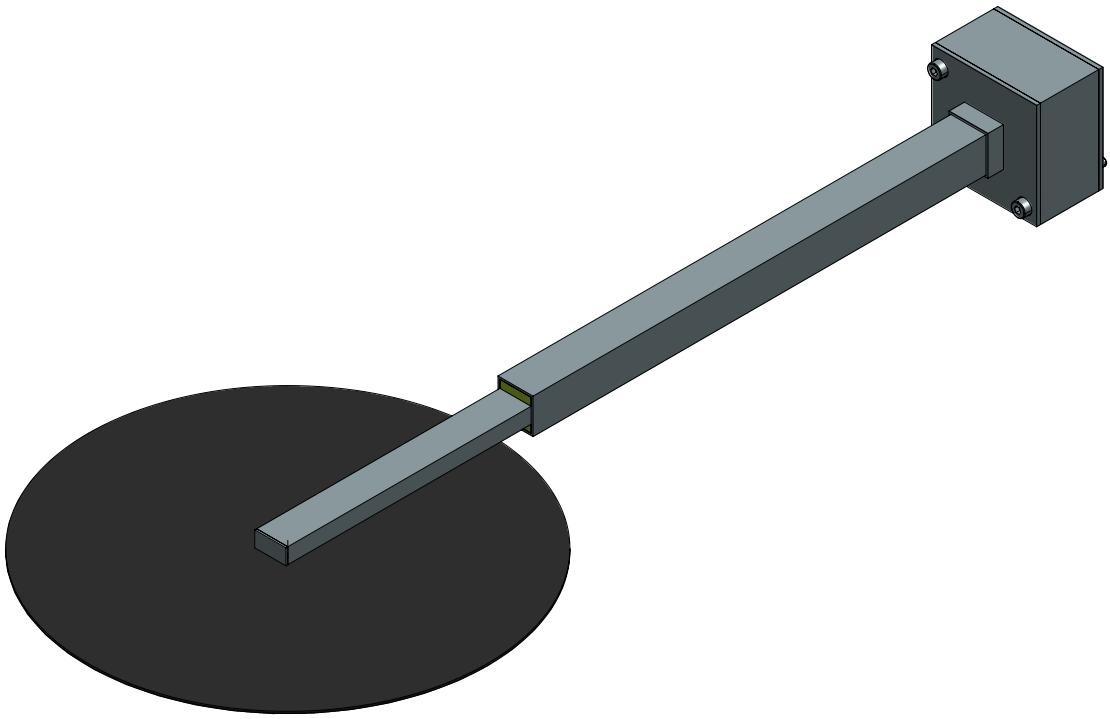

Figure 3.1: The design concept shown in isometric view

Distributing the force on the wafer surface is also possible with electrostatic handling, however an electrostatic handler builds large in height and the height for the design is limited to 10mm within the design space. The two other types of handling previously mentioned, bernoulli wafer

handling and mechanical wafer handling do not meet the requirements of supporting the wafer distributed on its surface [8][12][15], they have few local contact areas that can result in local force concentrations.
Figure 3.2 provides a sidebiew of the design concept, identifying its components.

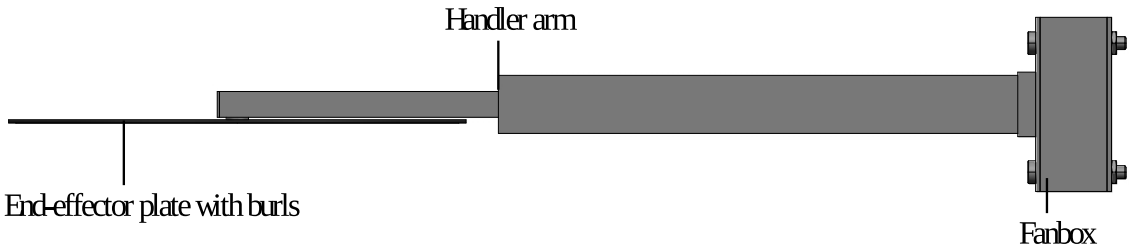

Figure 3.2: A side view of the design concept, identifying its components

Burls are used on the end-effector plate of the design concept to minimize surface area in contact with the wafer, preventing vanderwaals forces between wafer and end-effector, and therefore preventing the wafer sticking to the surface while supporting the wafer properly on its entire area. The burls will be further explained in section 3.2. They are manufactured on the bottom of the round carbon fibre plate ,with a diameter of 205 mm, and a hole in the middle for the air to go through,shown in the figure. This plate will be eleborated on in section 3.3. The end-effector plate and the handler arm are connected through a vertical round tube of diameter 10mm, with a hole for the air to flow through, dicussed in section 3.4. The handler arm, in section 3.5, will be the component placed on top of a z/θ-robot, which will perform the rotation and the z-stroke desired. The movement profiles for the wafer on the handler are given in 2.1. The wafer is displaced 550mm in the xy-plane by turning 90 degrees. The length of the arm is determined through the desired displacement. The handler arm connects the end-effector to the box on its other end, containing the fan used to create the under pressure, explained in section 3.6. In addition to the design concept, other options for the main functionalities are evaluated in appendix F.

Under pressure for thin wafer handling design concept

In order to determine the desired under pressure for the thin wafer, the wafer behaviour is analysed. In figure 3.3 the forces that can act on the wafer are represented.

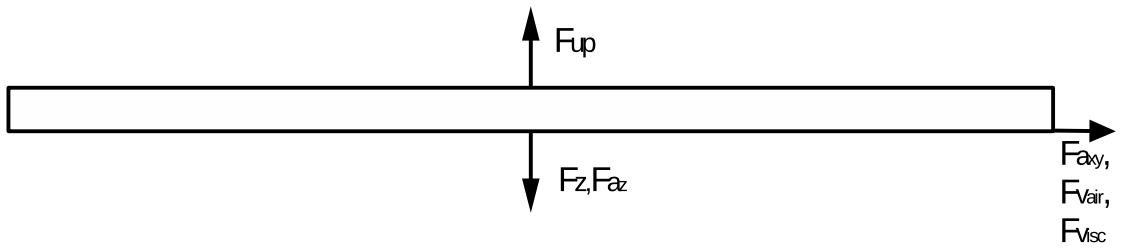

Figure 3.3: Force balance of forces on the wafer

The forces acting on the wafer in z-direction are the gravity force of the wafer(F_z) and the force acting as a result of the acceleration in z-direction(F_{a_z}). The mass of the wafer is calculated with equation 3.1, with the height of the wafer. The gravity force is defined in equation 3.2 and the acceleration forces in equations 3.3 and 3.4.

$$m_{wafer} = \rho_{SI}\pi(r_{wafer})^2 h \tag{3.1}$$

$$F_z = m_{wafer} g \tag{3.2}$$

$$F_{a_z} = m_{wafer} a_z \tag{3.3}$$

$$F_{a_{xy}} = m_{wafer} a_{xy} \tag{3.4}$$

The mass of the wafer is $m_{wafer} = 3.7 - 5.2g$, corresponding to the thickness of $50 - 70\mu m$. The acceleration in z-direction is calculated to $a_z = 0.81 \frac{m}{s^2}$. The forces acting on the wafer in the horizontal direction are the force due to the acceleration in this direction($F_{a_{xy}}$), the accelaration is $a_{xy} = 0.045 \frac{m}{s^2}$. The viscous forces of air act on the wafer when moving(F_{visc}) and the force of the dynamic pressure acts on the wafer as a result of the air speed moving along the wafer($F_{v_{air}}$), both when moving in the xy-plane. The density and viscosity of air are taken at $T = 20°C$ and are respectiveley $\rho_{air} = 1.2041 \frac{kg}{m^3}$ and $\mu_{air} = 1.8205e-5 \frac{kg}{ms}$. The formulas for the dynamic pressure and the viscous forces are shown in equations 3.5 and 3.6.

$$F_{visc} = \mu_{air} A \frac{v_{air}}{h_g} \tag{3.5}$$

$$F_{air} = \rho_{air} v_{air}^2 A \tag{3.6}$$

F_{up} is the force of the under pressure, which should always be larger than the sum of the previously mentioned forces. This sum is provided with equations 3.7 - 3.9, in these equations $\mu_{friction}$ is the friction coefficient between the silicon wafer and the viton burls, with a value of $\mu_{friction} = 0.2$.

$$\sum F = F_{vert} + \frac{F_{hor}}{\mu_{friction}} \tag{3.7}$$

$$F_{vert} = F_z + F_{a_z} \tag{3.8}$$

$$F_{hor} = F_{a_{xy}} + F_{visc} + F_{v_{air}} \tag{3.9}$$

Because an under pressure is used to create the force on the wafer, the pressure needed to hold the wafer can be determined through equation 3.10, with P the under pressure needed and A_{wafer} the surface area of the 200mm wafer.

$$P = \frac{\sum F}{A_{wafer}} \tag{3.10}$$

The under pressure needed to hold the wafer following from these equations is $26.2Pa$, as shown in section 2.1. The force of the under pressure should always be larger than the combined forces stated above. To account for any unforseen disturbances a safety factor of 3 is taken, bringing the desired underpressure between the wafer and the end-effector plate to $78.6Pa$, distributed on the wafers surface.

3.2 Burls on the end-effector

A solution to supporting a standard wafer, distributed over its surface area is a burl table [19]. A burl is a strut with typically a burl pitch of $3mm$, diameter of $25\mu m$ and a height of at least $0.15mm$[9][6], placed in a pattern to support a wafer.

Burl pattern

A recently developed burl pattern supports the wafer radially as opposed to previous patterns which were triangular or squared, and did not support the the outer radius of a wafer properly[19]. The pattern chosen is defined by the formulas in equations 3.11 and 3.12.

$$x_{i,j} = B_p i cos\left(\frac{2pi}{6i}j\right), \quad \text{with} \quad i = 0, 1, ..., \quad \left[\frac{r_{bo}}{B_p}\right], j = 0, ..., (6i-1) \tag{3.11}$$

$$y_{i,j} = B_p i sin\left(\frac{2pi}{6i}j\right) \tag{3.12}$$

This is a hexacircular pattern with an interdistance in radial direction called the burl pitch(B_p), a graphical representation is given in figure 3.4[19].

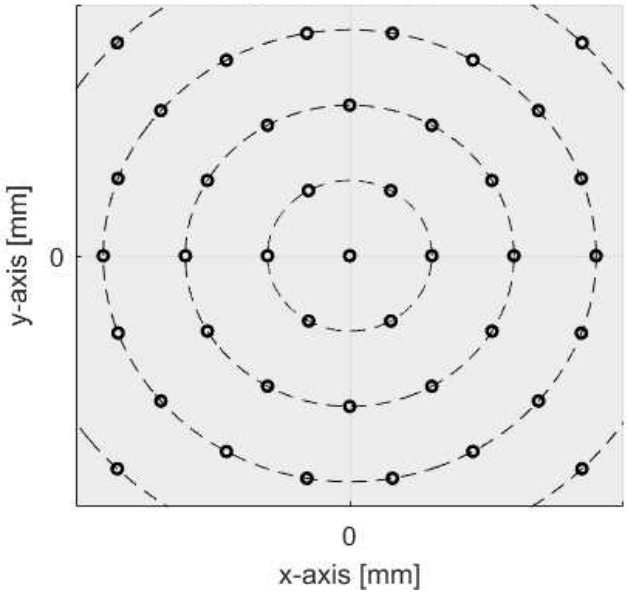

Figure 3.4: A schematic overview of the hexacircular grid used for the burls[19]

Wafer to burl behaviour

In figure 3.5 a partial axissymmetric view of a plate with burls and a wafer on the burls is shown, as well as the other parameters considered in the wafer to burl contact. These are the burl pitch(B_p), the burl radius(r_b) and the burl crowning(r_{cb}). h_B in the figure is the height of the burl.

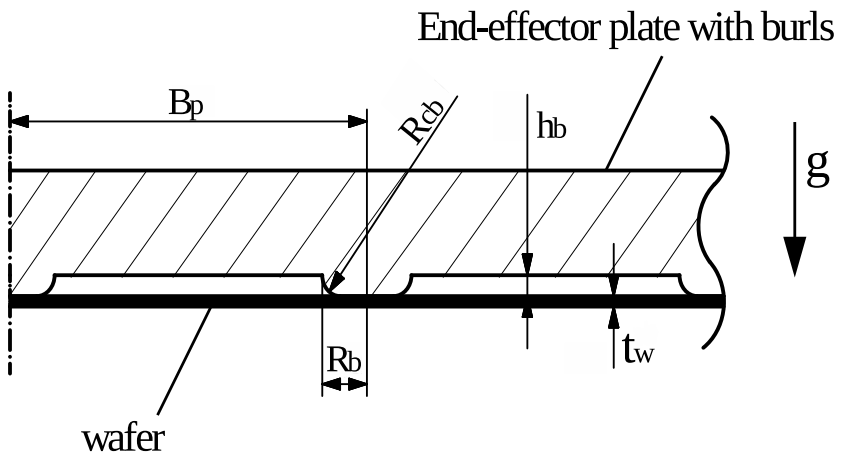

Figure 3.5: A schematic overview of a sectioned part of the end-effector plate with burls and wafer

The touching surface area of the burls with the wafer is dependent on the burl pitch and the burl diameter($D_B = 2r_B$). Determination of the burl pitch is done through deflection and stress calculation with the euler beam method for a piece of wafer, as shown in figure 3.6.

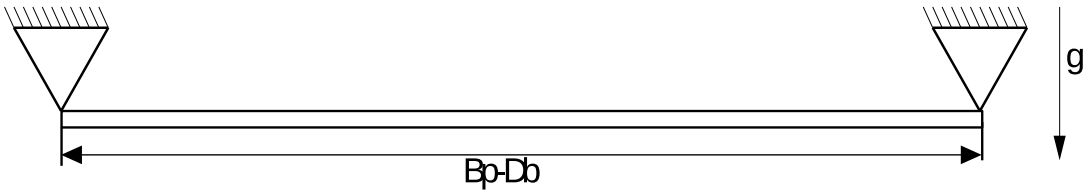

Figure 3.6: A schematic of a wafer section, simply supported on both ends

Other parameters taken into account in this euler beam analysis equivalent are the burl material and the crowning of the burl. The burl pitch range is $[5 : 5 : 30]mm$ and the burl radius range is $[0.125 : 0.125 : 1]mm$. The formulas for the deflection and stress in the centre of the modelled beam are stated in respectively equation 3.13 and equation 3.14.

$$\delta = \frac{5}{384}\frac{ql^4}{EI} \tag{3.13}$$

$$\sigma = \frac{Mc}{I} \tag{3.14}$$

The results for the stresses in the middle of the beam for varying B_p and p are shown in figures 3.7 and 3.8. The stress for varying burl radius is approximately a quadratic function, which is logical since the number of burls increases similar to a quadratic funtion.
The dependancy on the pressure for the stress in the middle of the beam is linear, which is obvious since they have a linear relationship.
The stress result for the varying r_b do not significantly change, as seen in Appendix B. The results for the deflection in the middle of the beam for varying B_p and p are shown in Appendix B.

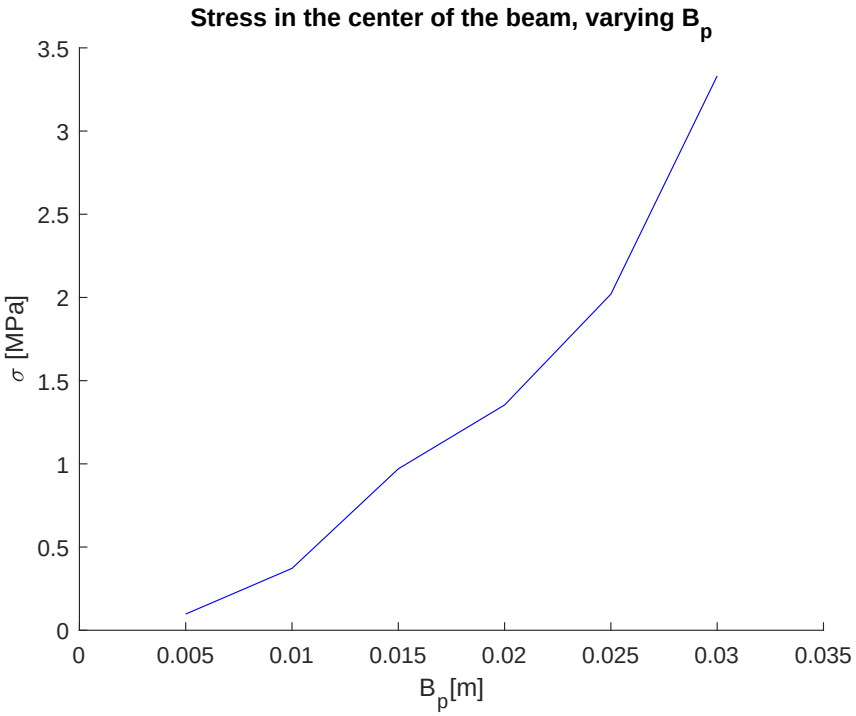

Figure 3.7: Results for the stress in the middle of the beam simulated piece of wafer for varying burl radius, burl pitch and pressure

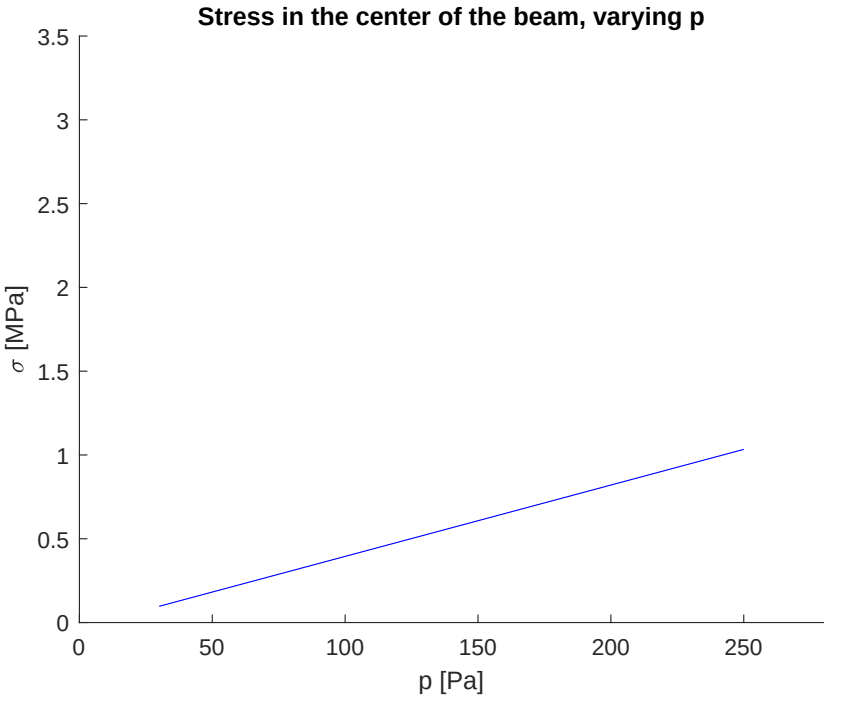

Figure 3.8: Results for the stress in the middle of the beam simulated piece of wafer for varying burl radius, burl pitch and pressure

The conclusions drawn for the dimensioning of the burls from the above calculations and simulations are as follows: the $B_p = 10mm$, the $r_B = 0.25mm$ and the determined pressure of $p = 78.6Pa$. These values are chosen since the stress remains well below the σ_{max}= $4MPa$ of viton. The B_p can be increased and the stress will remain below σ_{max}, however for a burl pitch of 10mm the total surface area for all burls is 0.2% of the total surface area of the wafer. The r_b is chosen this way because increasing the r_b means increasing the contact syurface area between wafer and burls.
The materials compared are SiSiC, a DLC coating(hardened steel), Viton and PEEK, since these are materials used, or applicable to be used, for burls[2]. The maximum allowable stress in silicon is lower than the maximum allowable stress in both SiSiC and hardened steel. If one of these materials is used, it will result in damage to the wafer. The maximum allowable stress in the PEEK and the viton is both lower than the maximum allowable stress in silicon. Peek is a hard plastic, while viton is a soft rubber, often used for o-rings and comparable applications. This is more in the line of what we want to use the material for and therefore the burls and seal are manufactured from viton. Figure 3.9 shows the configuration of the burls on the end-effector plate.

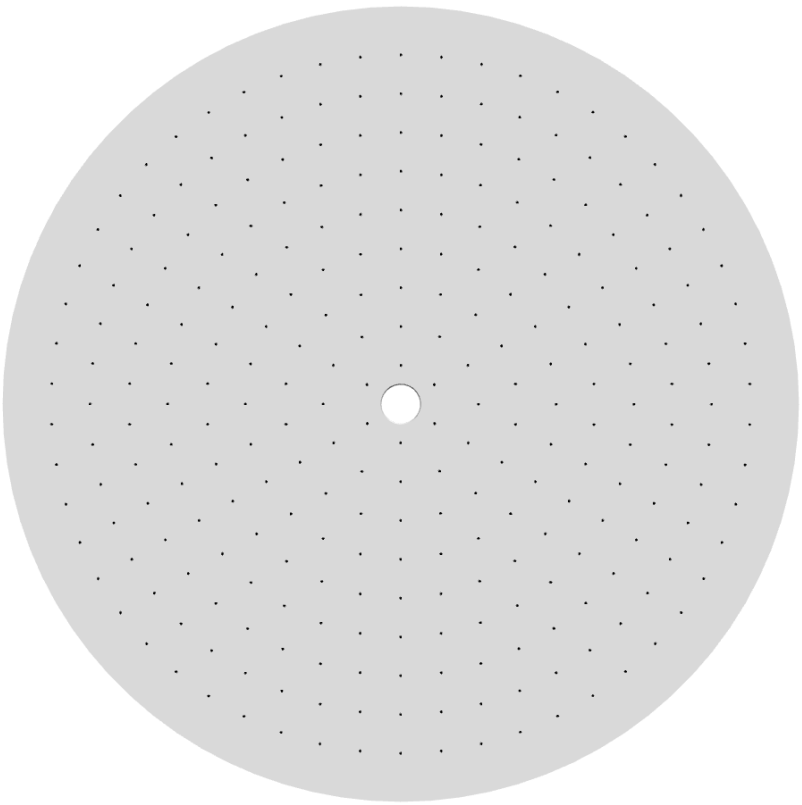

Figure 3.9: View of the burl pattern on the end-effector plate

Burl production

The fabrication process of the viton burls with a height of $50\mu m$, radius of $0.5mm$ and burl pitch of 10mm is silkscreen printing them on the end-effector plate. First the plate will be treated with a chemical compound to make the silkscreen printed material stick to it.
The other possibility for the fabrication of the viton burls on the end-effector plate would be to apply the viton to the plate and laser-cut the viton afterwards. Both methods have disadvantages, the silkscreenprinting is done in rectangular grids, so the burl will never be acutally round[23], being a possible cause for stress concentrations. When the viton is laser cut, first a foil of viton is stuck to the end-effector plate, after which the pattern will be lasered and the residu of the viton not needed can be removed. The laser-cutting unfortunately will melt part of the viton and has tolerances up to 0.05mm[13][24]. There are several companies[13][24][17] able to laser-cut the viton of this thickness, while silkscreenprinting of this material is not yet common practice. This is the reason to choose the laser cutting as the method of production for small amount or single piece production, with the recommendation of further investigating silkscreenprinting, since this will have less waste then viton, can be produced with less tolerances on the sizes and can be produced faster.

3.3 End-effector plate

The end-effector plate has the function of supporting the burls on which the wafer is held during handling. Different options for the end-effector plate shape and material are considered, shown in the morphologic overview of Appendix F. A top view of the end-effector plate is shown in 3.10.

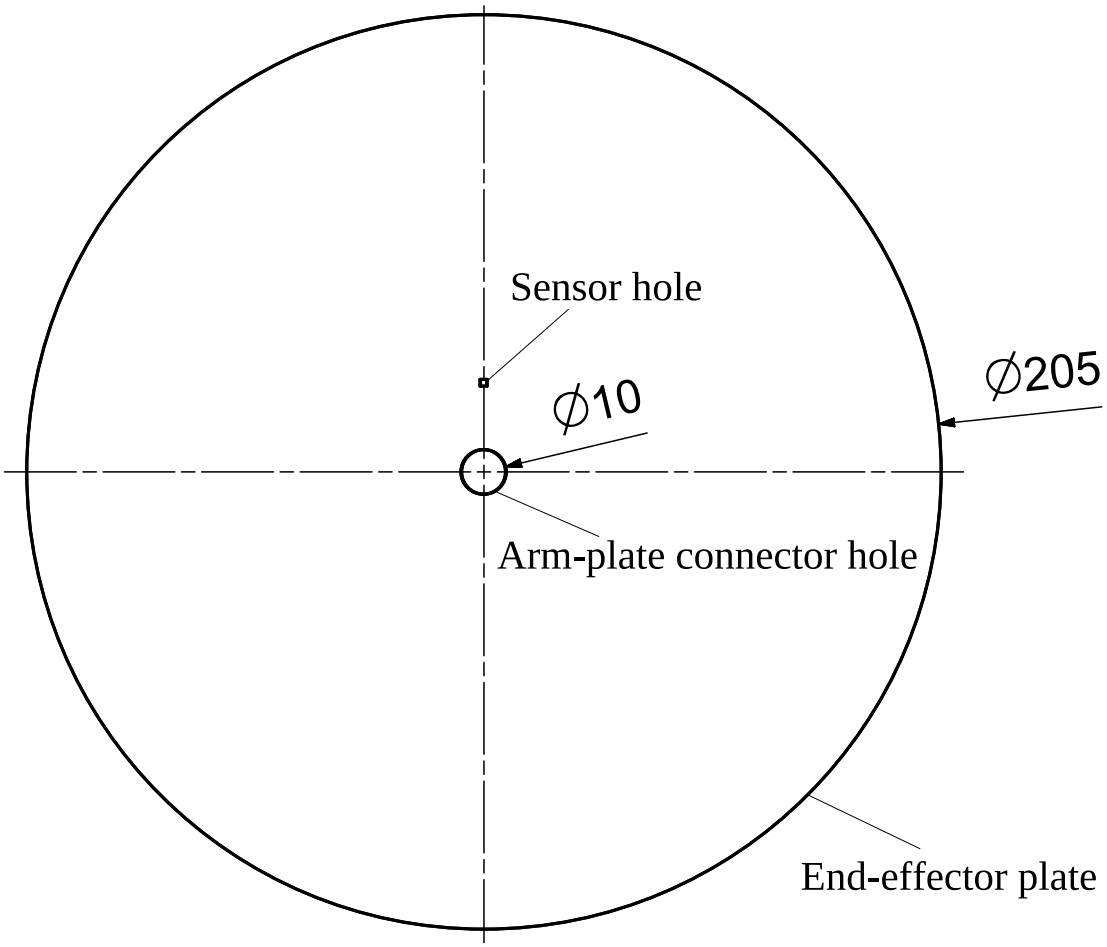

Figure 3.10: Topview of the end-effector plate

The maximum height available for the end-effector is 10mm, as previously mentioned in section 3.1, which should contain the burls, the end-effector plate and the arm connecting the plate to the robot and the fan. This maximum height in combination with the previously stated fact that the air pipe should be as large as possible for the least pressure drop in the pipe, concludes the plate should have little height. The mass of the wafer is only 3.7-5.2 grams, therefore the end-effector can also be very light, bringing the total mass needed for the robot down, and creating the possibility to have a simpler, more cost effective robot for the actuation.

Plate material

Materials compared for the end-effector are hardened steel, carbon fibre, aluminum and aluminumoxide. Their youngs modulus is compared to the density of the material in table 3.1.

	hardened steel	aluminum	aluminumoxide	carbon fibre
Youngs modulus $[GPa]$	207	69	300	138
density $[\frac{kg}{m^3}]$	7870	2700	3700	1550

Table 3.1: Youngs modulus and density compared for the possible end-effector materials[21]

This clearly shows that carbon fibre is the best option, stiffness to density compared. However carbon fibre is relatively expensive to process in comparison to for example steel or aluminum. An option to enlarge the stiffness further, when using carbon fibre, is the put every $50\mu m$ thin sheet of carbon fibre in a different direction, radially seen, to create the best possible grid of sheets for the carbon fibre in radial direction. This is a technique used in standard thickness wafer handlers, to increase the stiffness of the handler[2].

Plate shape

Cost and space are two important factors in the end-effector plate design, therefore first a solid flat plate is considered. Next to this solid flat plate it is also considered to have a two part end-effector, consisting of top and bottom part, with hollow inside or with ridges between the two parts, like vertical walls, to add stiffness in comparison to the hollow option, yet adding less mass than with the solid flat plate. The three options are shown in a schemtic section in figure 3.11, the top option is the solid plate, the middle option is the hollow plate and the bottom option is the plate with vertical ridges.

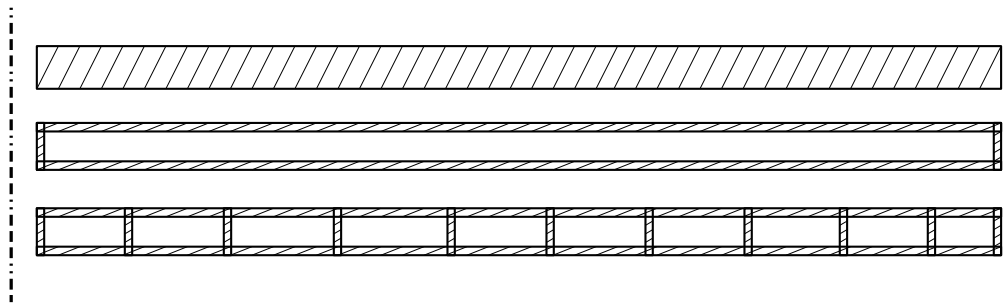

Figure 3.11: The three plate shapes compared in axissymmetric section view

Investigating the difference in the end-effector plate shape for a total hight of 1mm is done with an axissymetric simulation in comsol. In this simulation the deflection of the end-effector plate, under its own mass, is evaluated for the three previously mentioned options. In figure 3.12 this is shown, the deflection at the outer circumference is $26.1\mu m$ for the flat plate, $169.4\mu m$ for the hollow plate and $8.2\mu m$ for the plate with the vertical ridges.

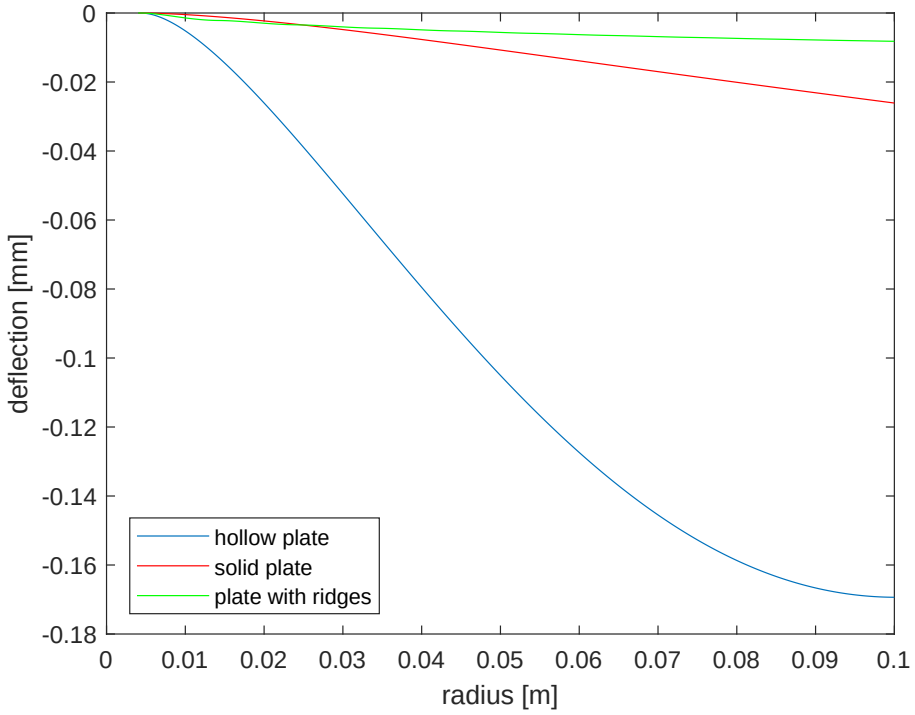

Figure 3.12: Deflection results of the plate shape simulations

The results of the deflection simulation show that the 1mm carbon fibre solid plate will deflect $26.1\mu m$ at the outer rim, under its own weight. To counteract this effect, the opposite line of figure 3.12 is taken as the axissymmetric shape of the end-effector plate during manufacturing. This way the end-effector will be flat when suspended above the wafer. This is achieved by creating the light curvature in the mold used for the carbon fibre production.
A carbon fibre object is manufactured by producing a mold that is the negative of the object[21]. Next the $50\mu m$ thin carbon sheets are layered in this mold and epoxy is added. The sheets are pressed together in the mold to get their form. The mold will then heat up to a temperature of $130 - 160°C$ and will have the slight curvature desired. One big plus of using carbon fibre is that the side that is pressed in to the mold is very flat, in the sence of surface flatness, and has very little particles on it after the fabrication process[2].
The flexural rigidity of the silicon wafer and the carbon fibre end-effector are determined, using equation 3.15, and compared.

$$D = \frac{Eh^3}{12(1-\nu^2)} \tag{3.15}$$

The flexural rigidty for the silicon wafer is $D_{wafer} = 1.47e-3$ and the flexural rigidity for the carbon fibre end-effector plate is $D_{EFplate} = 12.6$. The stiffness is defined as $\frac{EA}{L}$, which for the burl has a low L of $50\mu m$ and a high A, due to the number of burls. This results in a high stiffness for the burls in axial direction, because of this the stiffness of the end-effector plate can provide stiffness for the flexible wafer.
An eigen frequency analysis provides a first eigenmode with frequency $f = 181Hz$ for the plate, see Appendix C.

Seal

The end-effector plate is the base on which the burls are fabricated. The under pressure, with which the wafer is handled will be between the wafer and the end-effector plate. To handle the wafer with an under pressure of 78.6 Pa, the volume between the wafer and the end-effector plate is sealed. A zoomed in view of the seal on the end-effector plate is shown in figure 3.13.

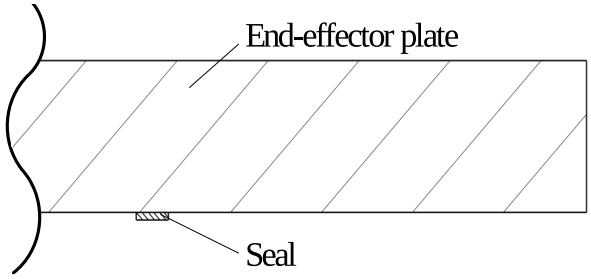

Figure 3.13: Detail section view of the end-effector with the seal

The seal has a height of $50\mu m$, similar to the burls, and a width of $0.25mm$ and is made of Viton. A bottom view of the end-effector plate with the seal as well as the burls on it is shown in figure 3.14. This seal, theoretically, ensures an air-thight volume between wafer and end-effector plate.

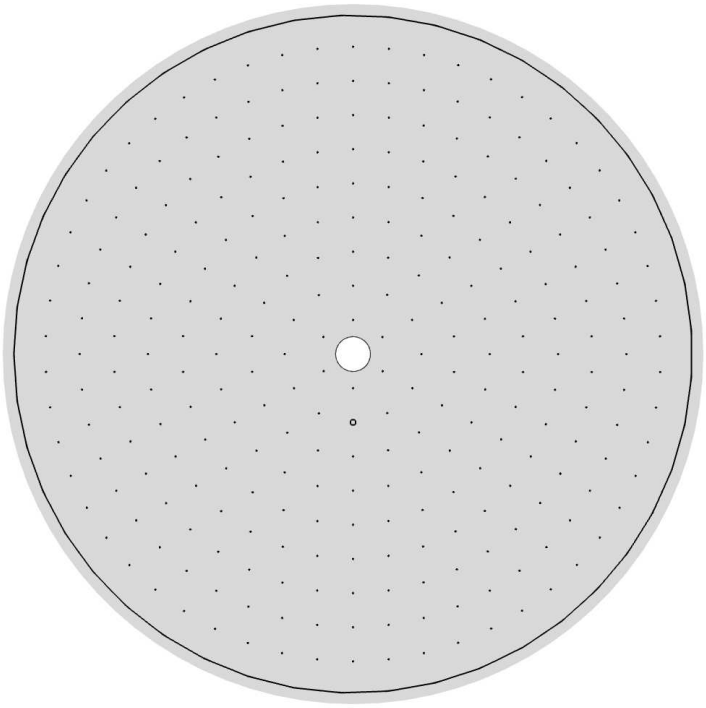

Figure 3.14: Topview of the end-effector platewith the burls and the seal

However a leak in the seal circumference can always happen and in practice some distance will always exist between seal and wafer. These effects are simulated in comsol, to verify leakages for which there is significant change in the under pressure in the volume between wafer and end-effector.

Flow analysis

The simulation made is a 2D axissymmetrical simulation, the geometry simulated is shown in figures 3.15 and 3.16. Figure 3.15 shows schemtically the volume between the wafer and end-effector. Figure 3.16 is a detail of the seal part of figure 3.15. The volume of the burls is not taken into account, because it is only 0.2% of the total volume.

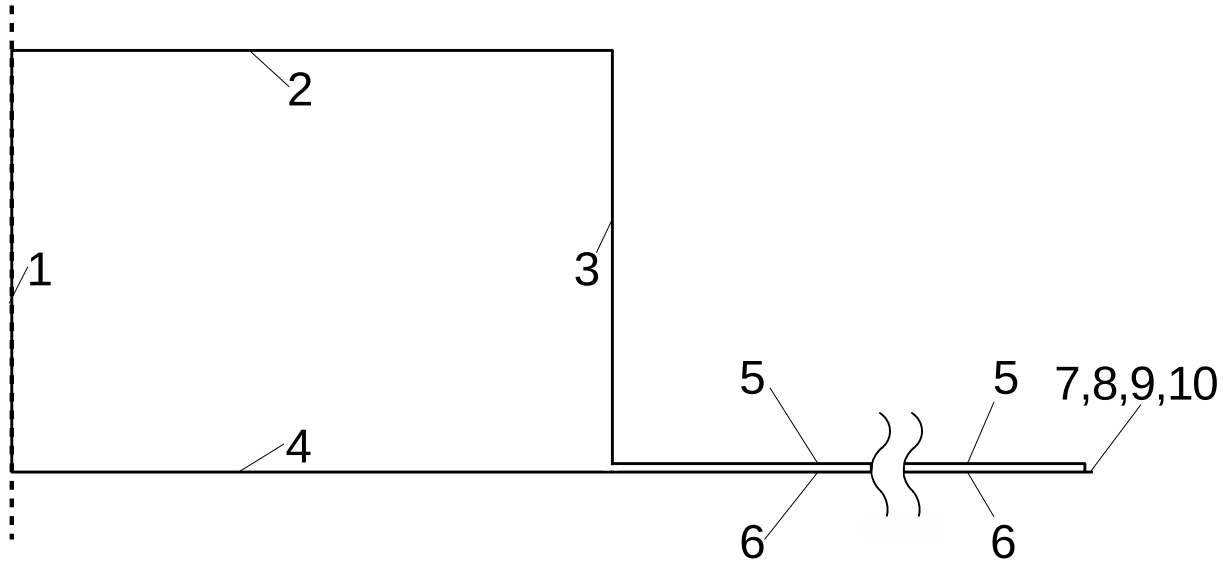

Figure 3.15: Schematic of the simulated area for the pneumatic comsol analysis

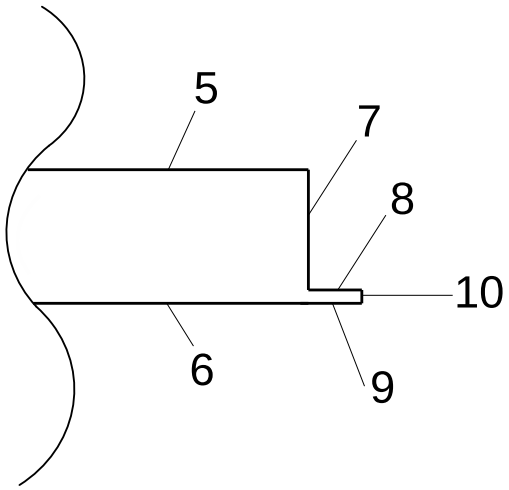

Figure 3.16: detail of the simulated area for the pneumatic comsol analysis

In these figures boundaries 3-6 define the physical boundaries for the air with respect to the end-effector plate/wafer. Boundary 1 is the axissymmetrical boundary because the simulation is axissymmetric. Boundaries 7-9 are the physical boundaries for the air with respect to the seal/wafer, this means boundary 8 is the length of the seal . Boundary 10 is the inlet in the simulation environment, this is the gap for the leakage defined. At boundary 2 a pressure is

defined to evaluate the pressure needed, at the point where the air flows from the vertical pipe for the end-effector support into the horizontal handler arm, with a pressure of 78.6Pa between end-effector plate and wafer.
The results following from this simulation are shown in figure 3.17, assuming a seal gap of 5μm and 4μm. In the figure it is shown that the pressure between the wafer and the end-effector is not uniform.

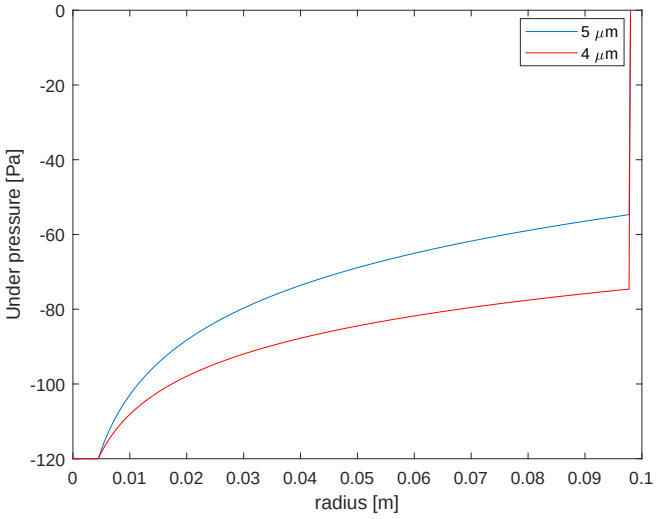

Figure 3.17: pressure non uniformity for the seal gap

To determine the seal gap with which the average pressure between the wafer and the end-effector plate is 78.6 Pa, the results from the comsol simulation are recalculated to the total force(F_{tot}) with equation 3.16.

$$F_{tot} = \sum P_N(A_N - A_{N-1}) \tag{3.16}$$

When this is calculated for the seal gap of 4μm, the total force is $F_{tot} = 2.47N$. The total force with a uniform distribution of 78.6Pa on the wafer area yields a force of $F = 2.46N$ therefore the seal gap of 4μm is desired.

3.4 End-effector plate to handler arm connection

The end-effector plate needs to be connected to the handler arm, with a mechanical connection as well as a pneumatic one. The mechanical connection should be axissymmetric, to ensure the wafer position with respect to the end-effector is not of influence to the load on the wafer. The pneumatic connection should be in the middle of the flat plate to have a radial flow between the end-effector plate and the wafer, equal in axissymmetric direction. These two combined dictate that the end effector plate to handler arm connection is situated in the middle of the end-effector plate.
In pneumatics usually bends are used to change the direction of a flow in a system with a pipe, however they are notorius for their pressure loss. In this case a bend is also rather difficult to execute practically, because the total height that the connection and handler arm can have is 8mm. It is chosen to have a vertical pipe, connecting the flat end-effector plate to the handler arm, of which a section view is shown in figure 3.18.

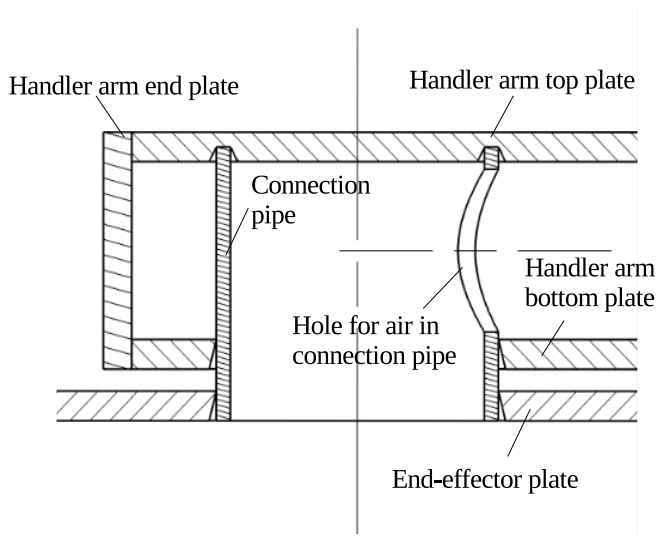

Figure 3.18: Section view of the vertical connection pipe between handler arm and end-effector plate

Pneumatics in the connection pipe

In the connection pipe, inner diameter $9mm$ and wall thickness of 0.5mm, a hole of $5.5mm$ is cut in the direction of the fan, to accommodate the air flow through the pipe. Figure 3.19 is an isometric view of the connection pipe with the hole of diameter $5.5mm$ visible, through which the air flows in the direction of the fan.

Connection points

The pipe wil be glued to both the end-effector plate and the handler arm, because it is a pneumatic system, it needs to be air thight. Also any deformation during assembly of the seperate parts should be prevented for the smoothness of the airflow, hence glueing the parts together. The connection will be made to the handler arm in two points. In the upper plate of the handler arm, the pipe will be glued on its inner and outer circumfurence. This will be done by applying the glue to the inside and outside of the tube and then place the tube inside the plate of the handler arm. Figure 3.20 shows the top connection to the handler arm.

Figure 3.21 shows the glued connection to the bottom plat in the handler arm, this connection is

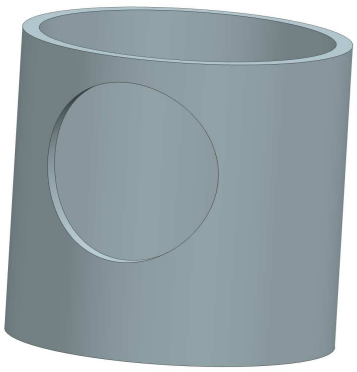

Figure 3.19: Isometric view of the vertical connection pipe

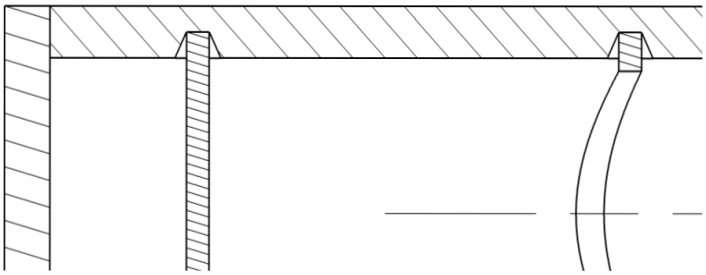

Figure 3.20: Section view of the vertical connection pipe to handler arm top plate connection

made on the outer cicumference of the vertical connection pipe.

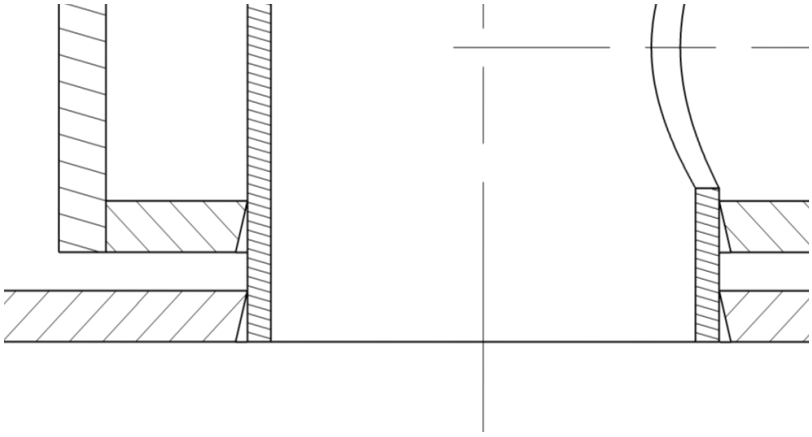

Figure 3.21: Section view of the vertical connection pipe to handler arm bottom plate and end-effector connection

The connection between the vertical pipe and the end-effector plate is shown in also shown in this figure. These connections will both be made in the same way as the glueing to the top plate of the handler arm, the glue is applied to the connection pipe and the connection pipe is placed inside the plate.

3.5 Handler arm

The handler arm is used to connect the end-effector with the fan, inside the fanbox at its end. It is also the connection with the r/θ-robot. The handler arm is shown in figure 3.22.

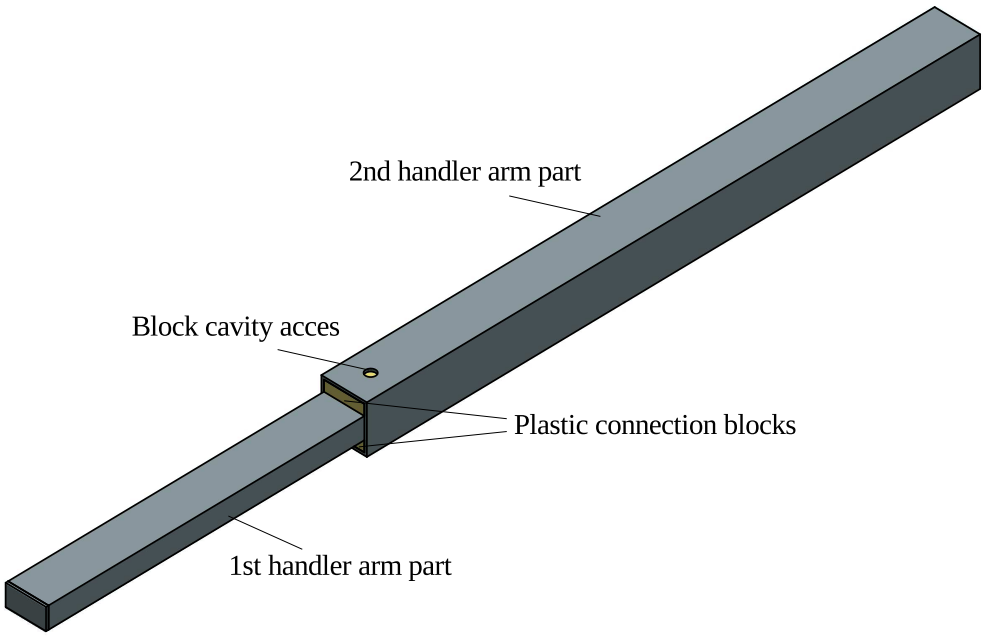

Figure 3.22: Isometric view of the handler arm

This arm has four components: the "1st handler arm part", connecting to the end-effector plate via the vertical connection, the "2nd handler arm part", connecting the arm to the fanbox and the r/θ-robot, and the plastic connection blocks, which are used to glue both parts together. For the design of the handler arm, various shapes as well as materials are considered. The most important for determining the shape, are the stiffness and the hydraulic diameter of the arm, since it functions both as mechanical component as well as pneumatic component. The bending stiffness of the arm is dependent on its shape.
The hydraulic diameter, see equation 3.17, is the effective diameter of a flow, used to unify calculations to fit the equations of a circular tube, which are standard in pneumatic calculations. In this equation D_H is the hydraulic diameter, A_{flow} is the surface area of the flow and P_{flow} is the perimeter of the flow area.

$$D_H = \frac{4A_{flow}}{P_{flow}} \tag{3.17}$$

1st arm part

As previously mentioned the height available for the arm above the end-effector plate,within the design space, is 8mm. The rectangular shape, with a width of $16mm$, a height of $8mm$, with a plate thickness of $1mm$, and a hydraulic diameter of $D_H = 8.4mm$, is easy to manufacture and compatible to stock components.
The length of the first arm part is $L = 137mm$, concluding the pressure drop in the 1st arm part , using equation 3.18. This requires the air velocity during the volume displacement, which will be further discussed in section 3.6

$$\delta p_{arm} = \frac{32L\mu_{air}v_{flow}}{D_H^2} \tag{3.18}$$

The rectangular handler arm design with the same cross section on its length is evaluated in Appenix D on its eigenfrequency, which is $f = 30.2Hz$ for the 1st eigenmode, which is in bending. Because of the low bending stiffness for the arm in this configuration, adding more width is evaluated, since the height is limited by the design space. This proves to have a maximum between added stiffness and added mass for the eigenfrequency, equation 3.19 . Therefore the width of the rectangular tube is left at $16mm$.

$$f = \frac{1}{2\pi}\sqrt{\frac{k}{m}} \tag{3.19}$$

2nd arm part

Because the design space only limits the height of the design in the area of the wafer, the possibility of adding bending stiffness by adding height in the second part of the arm is chosen, and with this increasing the first eigenfrequency to $f = 59.0Hz$.
The second arm part in the design concept has a height of $18mm$, similar to the width, increasing the bending stiffness of the arm. This arm part also has plates of thickness $1mm$. The hydraulic diameter for this arm part is determined to $D_H = 16mm$. The length of this arm part is $L = 233mm$. The pressure drop in the second arm part will be revisited in section 3.6

Arm parts connection

The connection between the two arm parts, using the connection blocks, is shown in figure 3.23.

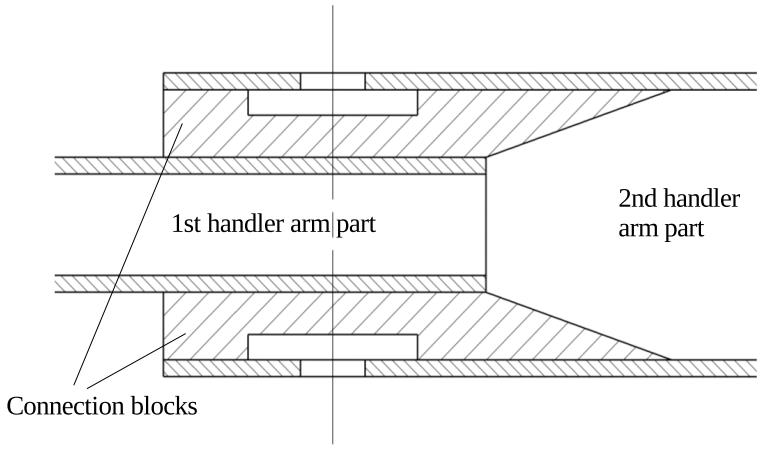

Figure 3.23: Section view of the connection between the 1st arm part and the 2nd arm part

The two arm parts are connect with two plastic inserts, glued to the first arm part , and slid into the second. To ensure airthightness, the platic inserts have a cavity, which will be purred through a hole in the second arm part, which are both shown in figure 3.23. In figure 3.24 the plastic insert is shown in isometric view.

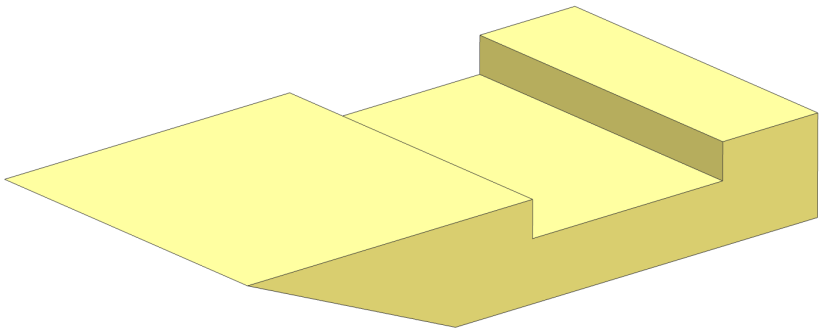

Figure 3.24: Isometric view of the plastic insert used to connect the two arm parts

3.6 Fan and fan box

The fan is originally meant for servor room useage and is a brushless fan with ball bearings inside.

Fan

The fan is used to create the desired under pressure of $78.6Pa$ between wafer and end-effector, it is a 50x50x20mm HHD brushles fan from MOUSER, shown in figure 3.25.

Figure 3.25: The 50x50x20 HHD Fan from MOUSER used to provide the under pressure

The fan creates an under pressure in the fanbox, handler arm and between the wafer and the end-effector, by displacing air from inside the volume to outside. From the δp determined on the top of the end effector, one can assume the under pressure desired at the fan is in the range of 120-130 Pa. With this information the 50x50x20HHD fan is decided on. An airflow/airpressure sheet is supplied with this fan, see Appendix E. The desired pressure at the fan of 120-130 Pa matches in this graph with a volumetric flowrate of $Q = 0.05\frac{m^3}{min}$.
The velocity of air is determined with equation 3.20. The hole in the vertical connection pipe is used to calculate the A. This will results in the highest possible velocity of air and therefore pressure drop in the handler arm, in accordance with equation 3.21. The velocity determined is $v_{flow} = 35\frac{m}{s}$, the pressure drops in the first and second arm part are calculated and are $\delta p_{arm1} = 0.04Pa$ and $\delta p_{arm2} = 0.02Pa$. The desired under pressure at the fan is then 120Pa.

$$v_{flow} = Q/A \tag{3.20}$$

$$\delta p_{arm} = \frac{32L\mu_{air}v_{flow}}{D_H^2} \tag{3.21}$$

The time it takes the fan to displace the volume is determined with the ideal gas law, see equations 3.22 and 3.23, with $\delta V = V_1 - V_2$. This gives a theoretical time of $t_{vol} = 6.8e-5s$ for the volume to be displaced when the wafer is adjoining the seal and the fan is on its required RPM.

$$p_1V_1 = p_2V2 \tag{3.22}$$

$$t_{vol} = \frac{\delta V}{Q} \tag{3.23}$$

One thing not taken into account here is the time it takes for the fan to get to its rotational speed desired.

Off the shelve solutions for creating an under pressure use reduction valves. Reduction valves are commercially available, but build large to get to an under pressure of 80 Pa, if they can produce this steady. Creating an under pressure of $78.6Pa$ accurately prooves rather difficult this way. Two simpler options to build a small under pressure with respect to the surrounding pressure are a pitot tube or a fan, creating an airflow out of the system.
A pitot tube creates an airflow by blowing higher velocity air into a tube, by means of a smaller tube, in one direction, creating a flow that also pulls the air besides the smaller tube with it. The pitot tube is further evaluated in Appendix F, the reason this is not the chosen way of creating the under pressure, is that reduction valves are needed in this case for this application as well.

Fan box

The fan box is the box atteched to the end of the handler arm. In this box the fan is mounted. Figure 3.26 shows a section of the fan box with the fan inside. The blue arrows indicate the direction of the flow respectively from the handler arm towards the surroundings.

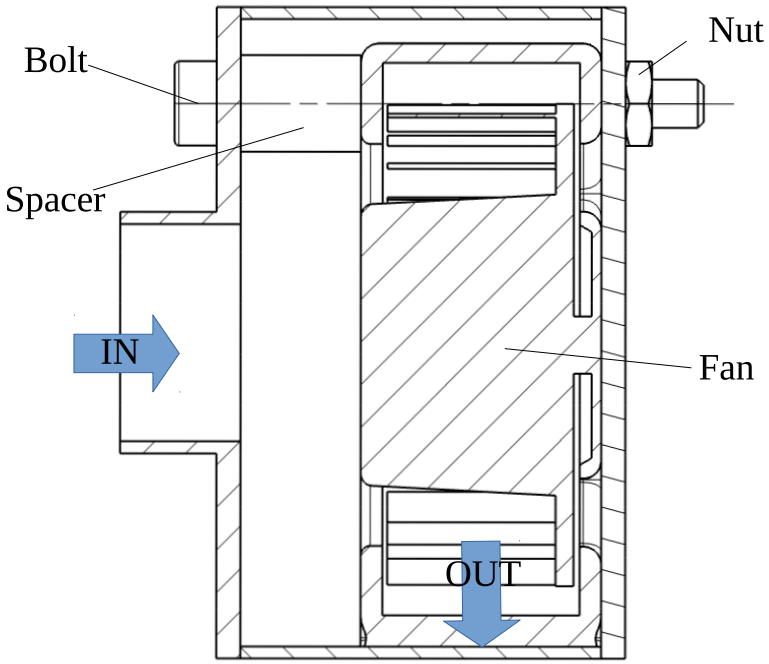

Figure 3.26: Section view of the fan box with the fan mounted. The fan box has an opening in the bottom for the air to go out by the indicated arrow.

The seperate components holding the fan in place are indicated in this figure. The fan is glued to the back plate, after which both plates are glued. Next the fan is bolted together with the fan box, with spacer in between. The spacers are in the fan box to provide space for the fan to suck the air out of the handler.

3.7 Design concept analyses

In this section the manufacturability, assembling, static behaviour and estimated handling time are considered in combination with the discussed/chosen components.

Design for manufacturing

The design concept is developed with an eye on costs, both in the components used as well as the manufacturing steps necessary for the production.
The arm and the fan box are manufactured from aluminium profile cut in pieces, with aluminum end caps that can be water cut from plate material. The two bolts and nuts used to assemble the fan box are stock components. The vertical connection pipe is made from standard pipe, with the hole in it water cut as well. The plastic blocks connecting the two arm parts are water cut also, since this is a cost effective way of removing material.
The end-effector plate is the relatively expensive part of this design. The manufacturing of it however is done with a mold, meaning high start up cost, but relatively cost effective with large numbers produced. The viton burls are relatively expensive as well, since they are laser cut. Investigating silkscreen printing further should bring the costs for this down, since this is a cost effective way of producing the burls on the plate.

Assembling the design concept

The pneumatic thin wafer handler should be assembled into two parts, before assembling the entire design. First the burls are manufactured on the end-effector plate, this plate is then glued to the connection pipe, this is assembly part 1. An exploded view of the components for assembly part 1 is shown in figure 3.27.

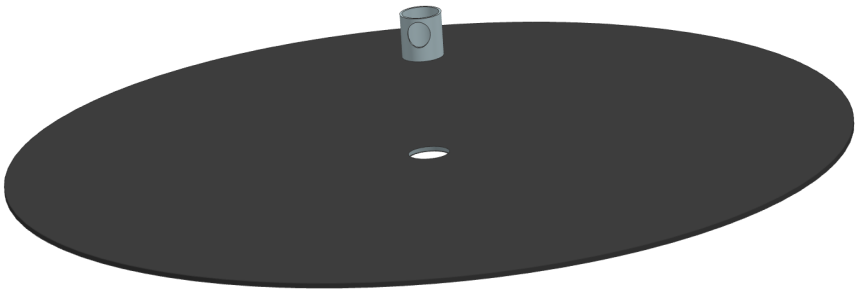

Figure 3.27: Exploded view of assembly 1

Assembly part 2 is assembled as follows: first the fan is placed in the tube and the end plates of the fan box are glued on, for airthightness and then bolted together. Next the plastic blocks are glued to the 1st arm part, glue is applied to the other side of the blocks and the 1st arm part with box is slid into the 2nd arm part. When the first and second arm part are assembled, to two holes in the second arm part are purred for airthightness. Now the fan box is glued on the 2nd arm part, forming assembly part 2 of the design concept. An exploded view of this assembly part is shown in figure 3.28.
Assembly part 1, with burls, plate and connection is then glued to assembly part 2, with the first and second arm part, the plastic blocks and the fan box.

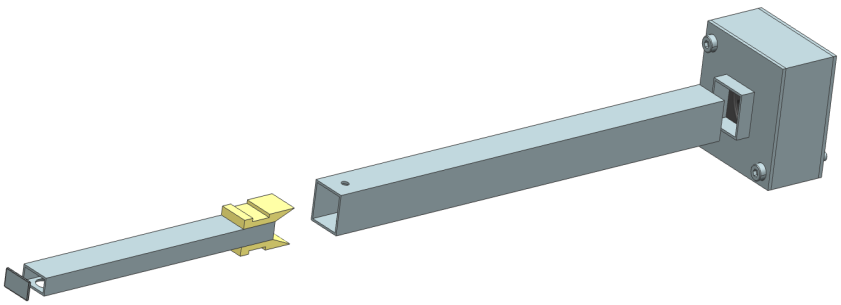

Figure 3.28: Exploded view of assembly 2

Eigen frequency analysis of the design concept

The Design concept is eveluated with an eigen frequency analysis in NX Finite Element Analysis. This is done for the design concept and for the design concept with the wafer mass added. There is no requirement on the frequency of the 1st eigenmode, though an eigenfrequency over 45Hz is prefered.
First the case without the added wafer mass is evaluated. The stress plot for the first eigenmode is shown below, in figure 3.29. The 1st eigenfrequency in this case is $f = 59.0Hz$, the displacement figure is shown in Appendix D. In the figure below the red circle indicates the area where the stress is the highest. Figure 3.30 is the zoomed in simulation result view for this areas.

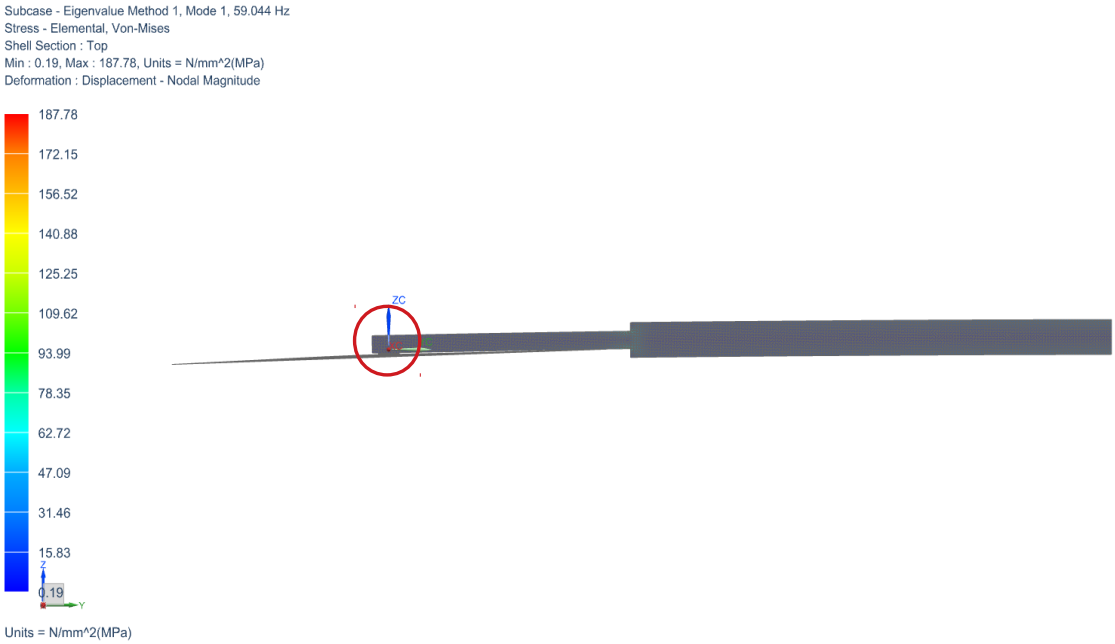

Figure 3.29: FEM result for the 1st eigenmode of the design concept

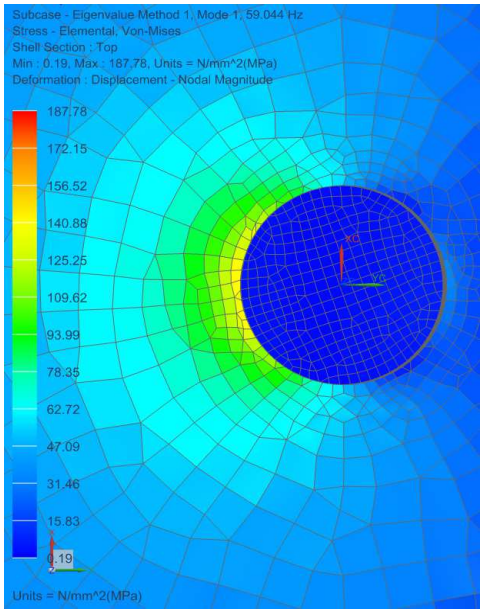

Figure 3.30: Zoomed in view of the FEM result for the 1st eigenmode of the design concept

The 1st eigenfrequency for the case with the added wafer mass is $f = 56.4Hz$, the simulation result figures are shown in Appendix D.

Wafer pick time pneumatics

The pick up of the wafer is determined using the comsol simulation previously mentioned in section 3.3. This simulation is altered for boundaries 4,6 and 9(figure 3.15, 3.16), enlarging the gap between the wafer and the end-effector. The gapheights simulated are $10, 20, 50$ *and* $100\mu m$, the under pressure results of these simulations are represented in figure 3.31.
From this graph is concluded that the average pressure in the outer 10mm of the radius, for gapheights of 50 and $100\mu m$ is $P_{HT} = 2Pa$. This value is used in equation 3.24-3.27 to determine the time it takes the wafer to adjoin to the seal. The value for the distance is $s = 100\mu m$, because this is the worst case scenario.

$$F_z + F_{a_z} = P_{HT} A_w \tag{3.24}$$

$$F_{a_z} = m_w a \tag{3.25}$$

$$a = \frac{P_{HT} A_w - F_z}{m_w} \tag{3.26}$$

$$t_{adjoin} = \sqrt{\frac{2s}{a}} \tag{3.27}$$

The time determined from these equation is $t_{adjoin} = .0052s$. This is a low estimate since the wafer will accelerate noticeably when the gap gets smaller. The total pneumatic pick time is defined in equation 3.28 and is $t_{pick} = 0.0053s$, with t_{vol} the time for the volume displacement determined in section 3.6.

$$t_{pick} = t_{adjoin} + t_{vol} \tag{3.28}$$

This concludes that the control of the fan is a major factor in the pick time and should be investigated.

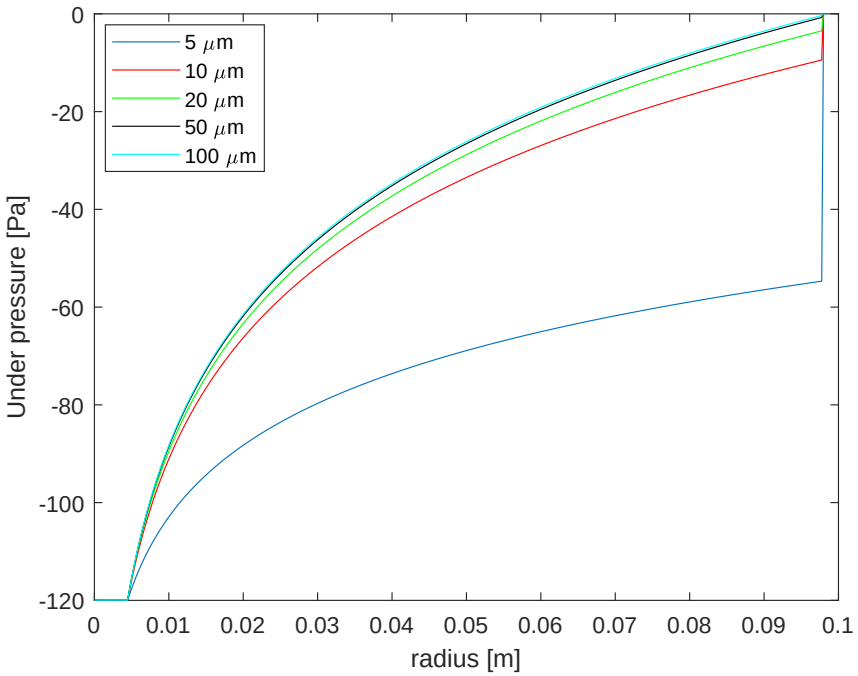

Figure 3.31: Simulation result for larger distance between end-effector and wafer during pick

Wafer place time pneumatics

The fan is shut down when the wafer is above the chuck for the place movement. Since the volume of air displaced to create the under pressure it is assumed the natural flow of air will restore the volume in the handler within the 1 second available for the pneumatics of the place movement.

Conclusion

The pneumatic thin wafer handler is able to pick, move and place a wafer within the required time using an under pressure of $78.6Pa$, distributed over the entire wafer surface without touching the edges or creating stress concentrations in the wafer. The handler can withstand the required accelerations and velocities stated in section 2.4. The wafer can be transfered from the chuck to the handler within 1 second. The eigenfrequency of the 1st eigen mode of the handler is 59.0 Hz without the wafer and 56.4 Hz with the wafer mass added, which is comfortably above the 45 Hz aimed for.

Recommendations

One recommendation made is to further investigate the production method of the viton burls on the end-effector plate. Silkscreen printing could be a more cost effective way of producing the burls on the end-effector plate.
When developing the controller for this thin wafer handler the start and stop times for the fan to reach its desired RPM should be taken into account, to limit the time for this step.

Chapter 4

Proof of design concept

This design concept,though verified with calculations and simulations, will have a test setup to prove its function.

4.1 Tests and context for the thin wafer handler test setup

Proposed test functionalities

The most critical part of the pneumatic handling of a thin wafer, with the handler design concept presented in this thesis, are the pick-up and place moments. A test setup for the thin wafer handler using an under pressure of $78.6Pa$ should be able to prove the following:

- The wafer can be picked up and placed with the handler. When the handler is placed on a z/θ-robot, it should also do the movements described in 2.1 in the xy-plane.
- The handling movement is possible with the same movement profile as the actual movement will have in z-direction, and in the xy-plane when the handler is placed on a z/θ-robot.
- The handling movement is repeatable with an under pressure of $78.6Pa$.
- The under pressure applied to the wafer, by the handler, is adjustable in at least the range of $50 - 100Pa$.
- Measure the under pressure between wafer and handler with respect to the atmospheric surroundings.
- Actively control the under pressure to the desired under pressure of 78.6 Pa.

Context for the test setup

Since the most critical part of the pneumatic thin wafer handling is the pick and the place movement, these are the main goal of the test setup. In this test setup, the thin wafer handler is placed above a TSU, shown in figure4.1. The TSU is a pneumatic wafer table. The TSU is able to clamp a wafer by being an air bearing with respect to the wafer[2]. The TSU can clamp the wafer, it can also provide a puff of air in the middle of the wafer, to release the wafer.

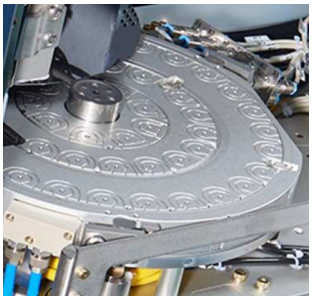

Figure 4.1: TSU wafer chuck

The TSU is able to displace in the z-direction with a distance of 0.1mm towards/away from a handler placing a wafer on it[2].
With the TSU and the handler prototype placed hovering over it in the test setup, a wafer can be picked up and placed on it. As previously shown in section 3.7 the handler will be able to pick up the wafer at a distance of 0.1mm, especially when the wafer is blown off the TSU, towards the handler.
The handler for the prototype will be similar to the design concept handler. For convenience it will be made from stock components that can be ordered per piece and since it will not have to displace the wafer in the xy-plane, the arm will be shorter.

4.2 Prototype for thin wafer handling

The prototype for the pneumatic thin water handler is based on the requirements for the design concept, proposed test functionalities and the context for the test setup, of section 4.1. The prototype is shown in figure 4.2. It is designed to be manufactured cost effective and with standard parts.

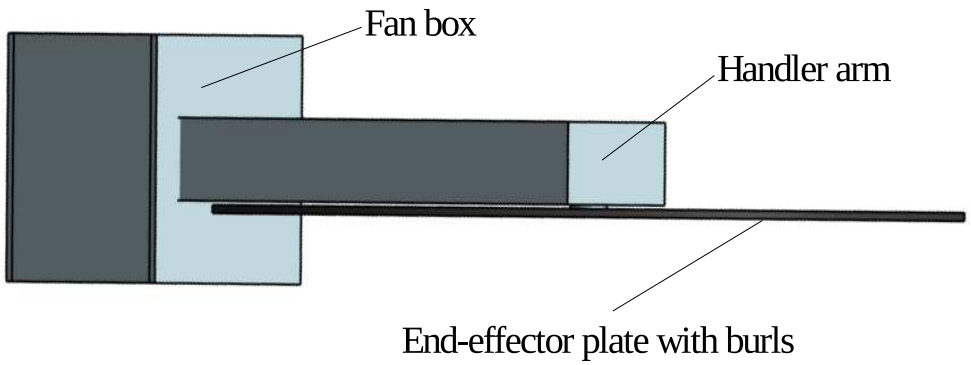

Figure 4.2: Isometric view of the prototype

The figure shows the prototype is very similar to the design concept. The differences are in the size of the components. One extra component with respect to the design concept is the dividing wall behind the fan. It is placed here to create a compartment for the electronics involved in the active control of the under pressure. This is shown in figure 4.3, where the components in the prototype are shown in a section view.

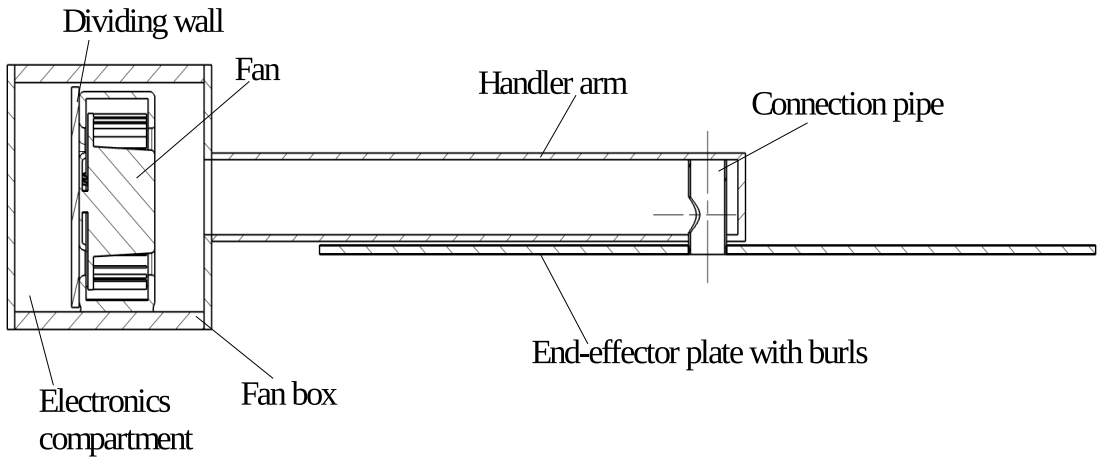

Figure 4.3: Section view of the prototype

In the following sections each of the components in the prototype is discussed, with respect to its twin in the design concept.

4.3 End-effector (3.2,3.3,3.4)

The end-effector contains the end-effector plate and the burls. Through the vertical connection the end-effector is connected to the handler arm. In the following subsections, the burls, end-effector plate and connection are shown for the prototype.

Burls and seal

The burls and the seal are manufactured on the prototype end-effector plate, with the same dimensions as for the design concept. The burl pattern is shown in figure 4.4 with the black dots, with the black circle in the figure being the seal.

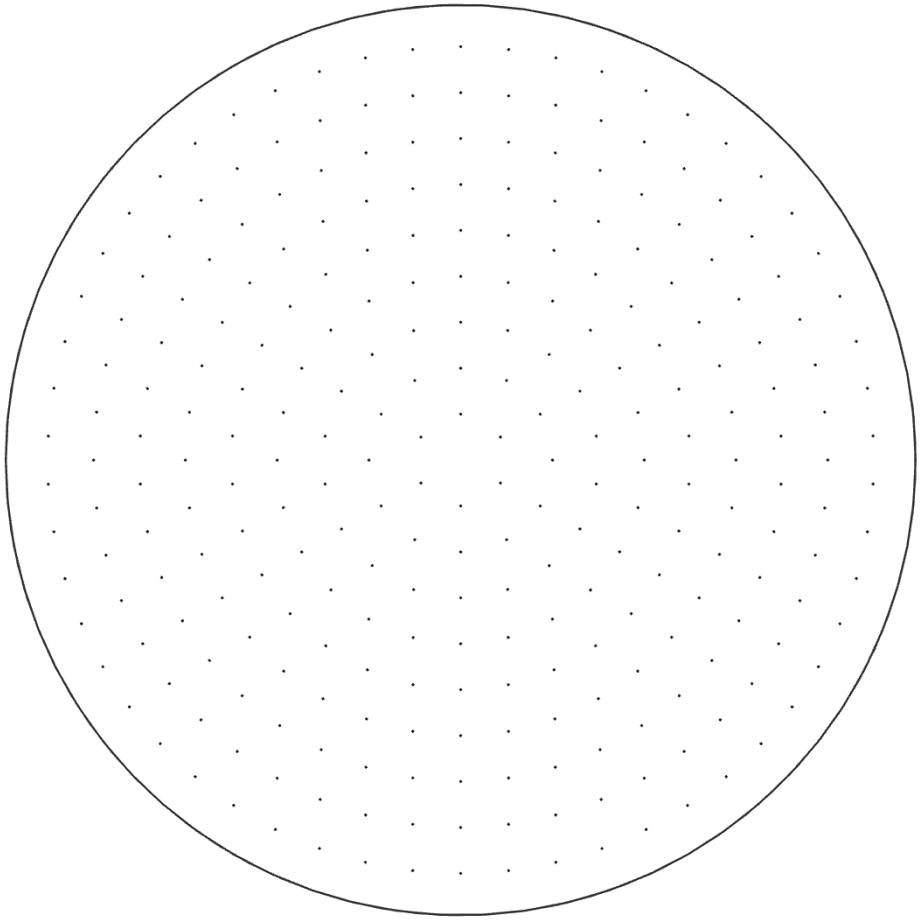

Figure 4.4: Burl pattern and seal

This pattern is manufactured by putting a plastic foil on the end-effector plate. This foil is then laser cut into the pattern shown above in figure 4.4.

End-effector plate

The end effector plate for the prototype is shown below from the top as well as from the side, figure 4.5. This plate has the same diameter as the end-effector plate of the design concept, $205mm$. The plate is however made from aluminum in this case, because this is more cost effective and is a stock component. An aluminum plate of the same thickness as a carbon fibre plate has a

different stiffness, as can be seen in table 3.1 comparing the Young's modulus and density. Similar stiffness of the plate for the aluminum is determined to be at $t = 1.25mm$, this is however not a stock thickness for these plates. Therefore the thickness of the plate for the prototype, as shown in figure 4.5 is $2mm$.

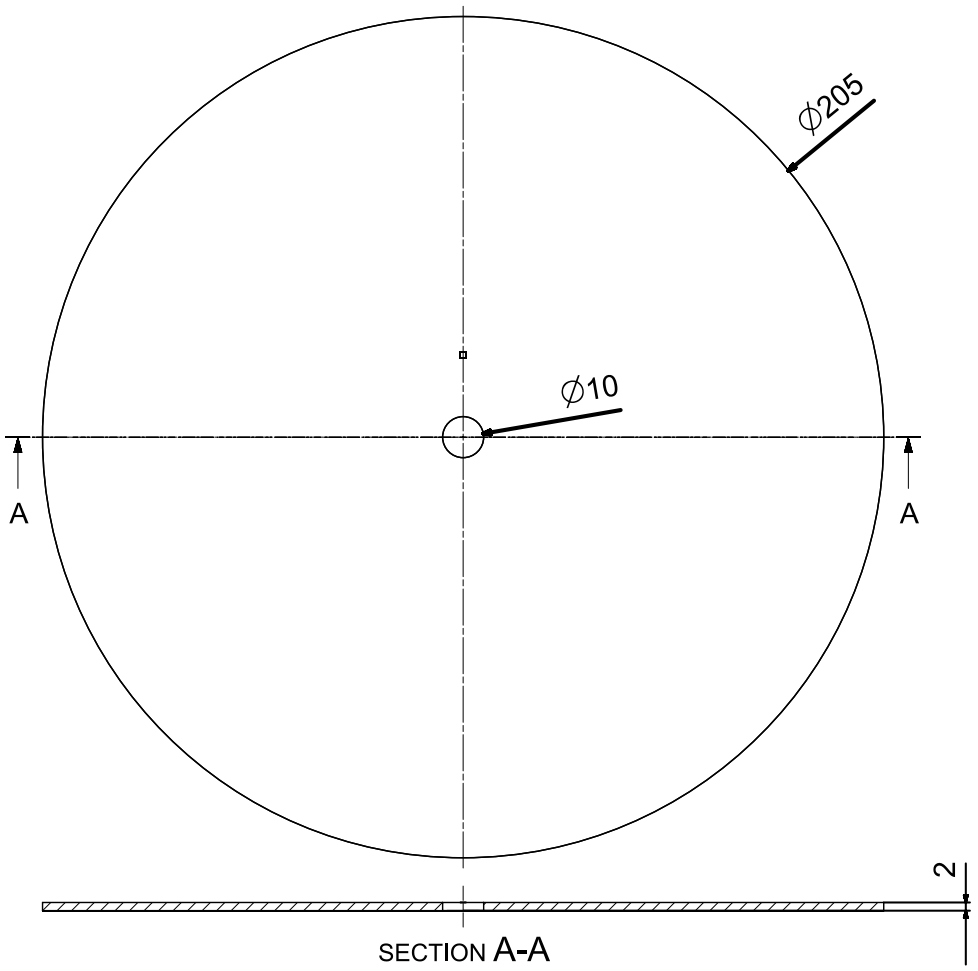

Figure 4.5: Top and section view of the end-effector plate for the prototype

The plate with diameter 205mm is manufactured from a flat squared plate of thickness 2mm. This plate is laser cut to the round shape with the desired diameter.

End-effector plate to arm connection

The end-effector plate to handler arm connection is similar to the one for the design concept. The connection pipe and a section view of the connection are shown below in figures 4.6 and 4.7.

Figure 4.6: Connection pipe of the prototype

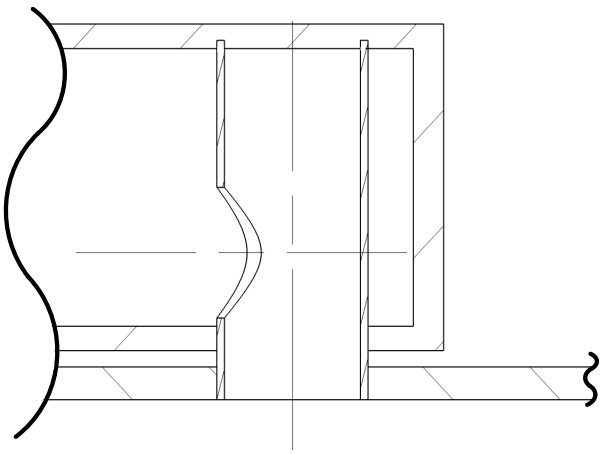

Figure 4.7: Section view of the connection pipe of the prototype

In this figures it is visible that the connection pipe in the prototype is longer than in the design concept. This is caused by the desire to use standard components, because of which the handler arm is larger in the prototype than in the design concept. This causes the connection pipe also to be longer. It is however the same diameter of 9mm as in the concept design and the hole in it remains $5.5mm$ for the prototype.

4.4 Handler arm of the prototype (3.5)

In this section the handler arm of the prototype and the fan box are discussed. A section view of the arm with the handler box glued to it, is shown in figure 4.8 with the dimensions.

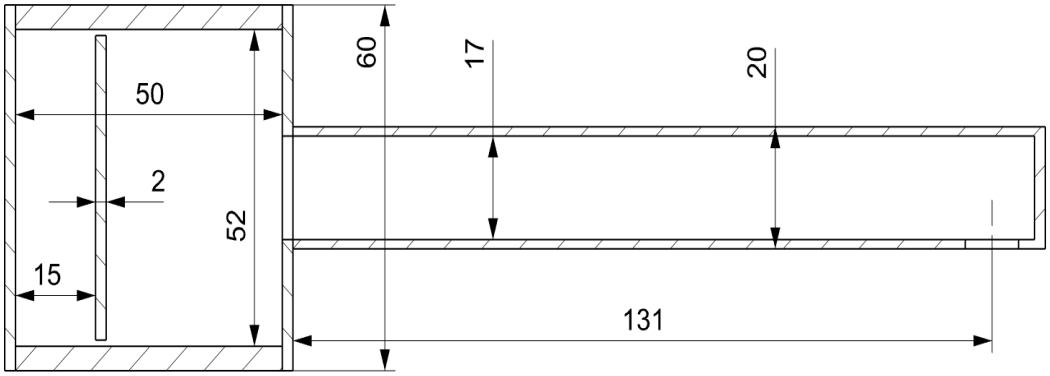

Figure 4.8: Section view of the prototype's handler arm

Handler arm

As opposed to the handler arm of the design concept, this arm is made out of 1 piece of standard tube, with dimensions 20x40x1.5mm. The end cap is cut from a plate of thickness 2mm.
The hydraulic diameter of the arm is determined with equation 4.1 to be $D_H = 23.3mm$. From this the $\delta p_{arm,proto}$ follows in accordance with equation 4.2. The velocity similar to the air velocity of the design concept, $v_{flow} = 35\frac{m}{s}$ gives the pressure drop in the arm, $\delta p_{arm,proto} = 0.0049Pa$. The desired under pressure at the fan is then 120Pa.

$$D_H = \frac{4A_{flow}}{P_{flow}} \tag{4.1}$$

$$\delta p_{arm} = \frac{32L\mu_{air}v_{air}}{D_H^2} \tag{4.2}$$

The handler arm is glued inside the plate connecing the fan box and the handler arm.

Fan box

The fan box is made out of standard tube with dimensions 60x60x4mm. A dividing wall is placed in the fan box, to have an electronics comopartment behind the fan. This is shown in figure 4.9. This dividing wall is glued in, as are the other plates of the fan box for the prototype. In the bottom plate of the fan box the outlet of the fan is situated, similar to the concept design.

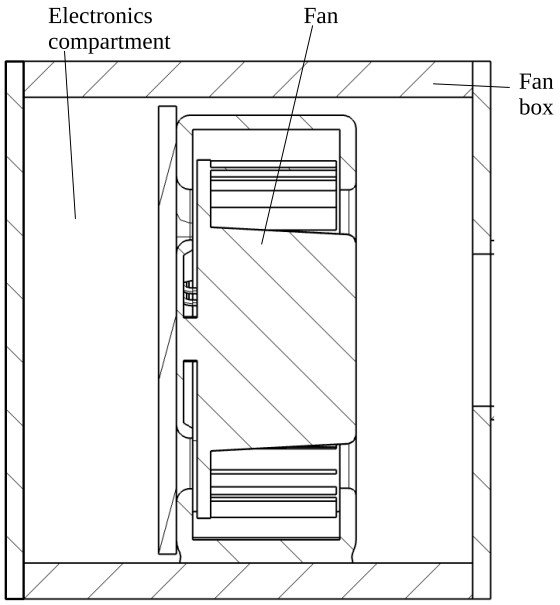

Figure 4.9: Section view of the prototype's fan box with fan and dividing wall

4.5 The fan and active control of the under pressure (3.6)

Fan

The fan is used to create the desired under pressure of $78.6Pa$ between wafer and end-effector, it is a 50x50x20mm HHD brushles fan from MOUSER, shown previously in figure 3.25.
The desired pressure at the fan is 120 Pa, similar to the design concept, with $Q = 0.05\frac{m^3}{min}$.
The time it takes the fan to displace the volume is determined with the ideal gas law, see equations 3.22 and 3.23, with $\delta V = V_1 - V_2$. This gives a theoretical time of $t_{vol} = 1.3e-4s$ for the volume to be displaced when the wafer is adjoining the seal and the fan is on its required RPM. This is an order of magnitude slower than the design concept, however still not significant for the handling times required. The t_adjoin is the same as for the concept design, bringing the total time to $t_{pick} = 0.0053s$.

Active control of the under pressure

The prototype has a sensor package placed on the radial position, where the average pressure of 80Pa is. This sensor package has one sensor measuring the atmosphere and one sensor measuring the pressure between the wafer and end-effector. This sensor is placed in the plate by drilling a small hole in the plate, placing the sensor in the hole and glueing it shut to prevent leakage.
With these sensors the prototype can be actively controlled,for instance with a PID controller, using an arduino connected to the sensors and the fan. This results in a adjustable desired pressure as well as active control of the fan to reach and stay on this desired pressure.

4.6 Prototype design

The prototype, opposed to the design concept, is assembled through glueing. First the dividing wall is glued inside the fan box. Next the fan is glued to the bottom of the fan box and the dividing wall. Then the plate connecting the fan box to the handler arm is glued to the fan box, after which the handler arm is glued to this plate. Simultaneously the viton foil is stuck to the

end-effector and the pattern for the burls and the seal is laser cut and the left over foil is removed from the end-effector plate. Now the connection pipe is glued to the end-effector plate. After this both sub-assemblies are glued together, by glueing the connection pipe to the top and bottom plate of the handler arm.
This assembly proces, with these components and the electronic components for the active control totals a cost of €30 − €40, dependent on where the components are bought and the machining of them is done.

Eigenfrequency analysis

The eigenfrequency analysis is also performed for the prototype, similar to the eigenfrequency analysis for the design concept. In figure 4.10 the stress in the prototype for the 1st eigenmode with eigenfrequency $f = 92.6Hz$ is shown, the highest stress occurs in the red encircled area. Figure 4.11 shows the zoomed in area with the highest stress concentration in the prototype in this first eigenmode.

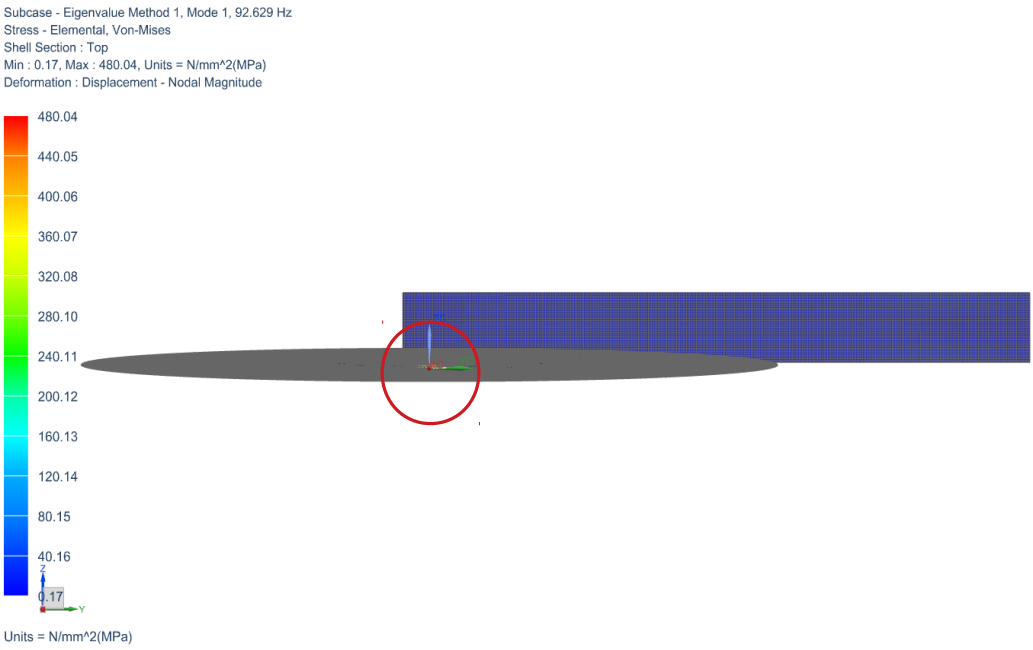

Figure 4.10: Eigenfrequency result prototype

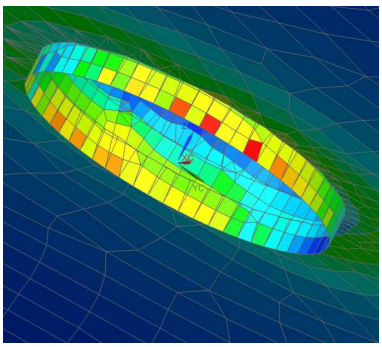

Figure 4.11: Eigenfrequency result prototype

Conclusion

The prototype will be able to perform the pick and the place movement desired. It is able to perform these movements within the time span stated by the requirements in section 4.1.
There are two pressure sensors measuring respectively the end-effector to wafer volume and the atmospheric surroundings, from which the under pressure can be determined as a difference between the two. The under pressure is actively controlled by means of the pressure sensors and an arduino with controller delivering feedback to the fan with respect to the desired pressure,adjustable within the desired range of section 4.1 , programmed into this arduino.
This concludes the prototype is able to perform the functionalities desired, within a very low budget.

Recommendations

Two recommendations with respect to the prototype are made.
The possibility to add a rotation actuator, holding the handler arm could be investigated, with the purpose to simulate the less critical xy-plane movements of the wafer handler with the wafer. This is not yet implemented because it increases the cost of the prototype, while not being the most critical property to be tested.
The second reccommendation is adding 4 pressure sensors to the prototype. Two sensor would be added axissymmetric, so three sensors would be under an 120° angle. This would be done to verify the axissymmetric uniformity of the under pressure. The other two sensors would be added in the radial direction, to verify the fluctuation in the under pressure towards the outside of the end-effector plate.
Adding these sensors however adds electrical cables and components to the prototype, to actively measure the pressures. It also increases the amount of work to program the active control for the pressure.

Chapter 5

Conclusion

In this thesis a pneumatic thin wafer handler is designed, able to gently handle $50\mu m$ wafers by providing only the minimal amount of force necessary. The thin wafer handler is able to pick, move and place a wafer within the required time using an under pressure of $78.6Pa$, distributed over the entire wafer surface. The main components of the design concept are the burls, end-effector plate, handler arm and fan, which are designed with cost effectiveness in mind. Furthermore the design concept can perform the requirements regarding accelerations, velocities and handling time.
To verify the design, a prototype is designed to perform the critical movements of pick and place. This prototype design proves the underlying idea of handling the thin wafer with minimal force.
Recommendations with respect to the design are to further investigate the burl fabrication process and to investigate the active control of the fan to reduce pick up and place time.

Bibliography

[1] SEMI M1-0414 - Specification for Polished Single Crystal Silicon Wafers. 2014. 1

[2] VDL confidential document. 2017. 1, 3, 5, 9, 16, 19, 20, 35, 36

[3] K. Bock C. Landesberger, S. Scherbaum. Carrier techniques for thin wafer processing . *CS MANTECH Conference*, 2007.

[4] DISCO Corporation. https://www.disco.co.jp/eg/solution/apexp/grinder/taiko.html, November 2017. 7

[5] Mr. Sumant Sood Dr. Shari Farrens, Mr. Pete Bisson and Mr. James Hermanowski. Thin Wafer Handling Challenges and Emerging Solutions. *ECS Transactions*, 2010. 1, 8

[6] Empel Tjarko, Rudolf van Adriaan, Koen Jacobus Johannes Maria Zaal, Aschwin Lodewijk Hendricus Johannes van Meer, Ton Aantjes . 13

[7] Wai Hong See Toh Justin et al. Evaluation of Support Wafer System for Thin Wafer Handling. *Electronics Packaging Technology Conference (EPTC)*, 12th, 2010. 1

[8] Euflex Technology Corp. http://www.euflex.com.tw/en/books/html/?164.html, November 2017. 7, 8, 11

[9] Guido De Boer, Michel Pieter Dansberg, Pieter Kruit , January 2018. 13

[10] H-Square corporation. http://www.h-square.com/Wafer_Mechanical_Picks.html, November 2017. 7, 8

[11] Infineon Technologies. https://www.infineon.com/export/sites/default/media/press/Image/press_photo/Infineon_300mm_Wafer.jpg, November 2017. 7, 8

[12] Innovative Robotics. http://www.innovativerobotics.com/site2011/Product-Wafer-End-Effector.html, November 2017. 7, 8, 11

[13] Interplate bv. https://www.interplate.nl/industriele-zeefdrukkerij/lasergraveren/, April 2018. 17

[14] J. Czochralski. *Ein neues Verfahren zur Messung der Kristallsationsgeschwindigkeit.* 1918. 1

[15] JEL Corporation. http://www.jel-robot.com/products/BERNOULLI_CHUCK.html, November 2017. 7, 8, 11

[16] Joachim N. Burghartz. *Ultra-thin chip technology and applications.* Springer, 2010. 1, 7, 8

[17] KJ Laser Micromachining Ltd. http://kjlasermicromachining.com/capabilities/laser-cutting/, April 2018. 17

[18] Zainuriah Hassan Michael Raj Marks and Kuan Yew Cheong. Ultrathin Wafer Pre-Assembly and Assembly Process Technologies: A Review. *Critical Reviews in Solid State and Materials Sciences*, 2015. 1

[19] M.M.A. Steur. *Design of an Active Wafer Clamp for Wafer Machines.* PhD thesis, TU/e, 2017. v, 13

[20] Nick Rosielle. *Design Principles for precise motion and positioning purposes.* TU/e, 2013. 7

[21] P.K. Mallick. *FIBERREINFORCED COMPOSITES:Materials, Manufacturing, and Design.* CRC Press, 2007. 19, 20

[22] Robert Doering and Yoshio Nishi. *Handbook of Semiconductor Manufacturing Technology, Second Edition.* CRC Press, 2008. 1, 7, 8

[23] Screen 70. http://www.screen70.nl/zeefdruk/, April 2018. 17

[24] Universal Laser Systems GmbH. https://www.ulsinc.com/resources/advanced-materials-processing-center/viton, April 2018. 17

Appendix A

Pneumatic thin wafer handling

Pneumatic thin wafer handling is divided in two separate cases. The first is when the principle of applying a vacuum/under pressure by suction is used to apply the normal force on the wafer. Second this normal force can also be exerted on the wafer by blowing out air, called the Bernoulli handler solution after Bernoulli's principle. Both solutions have a relatively low contact area with the wafer.
An example of a current thin wafer handling solution based on the principle of creating an under pressure by suction is shown below in A.1.

Figure A.1: An example of a thin wafer handling solution using vacuum to exert the normal force on the wafer.

These types of solutions are connected to a vacuum vessel and have several holes in their body through which the vacuum is created on the wafer. This vacuum has a relatively high Δp with respect to the atmospheric surroundings, resulting in a high normal force on the thin wafer. The normal force is then also applied locally, resulting in high stresses in the thin wafers.
Shown in A.2 is a schematic view of the standard Bernoulli wafer handling solution.

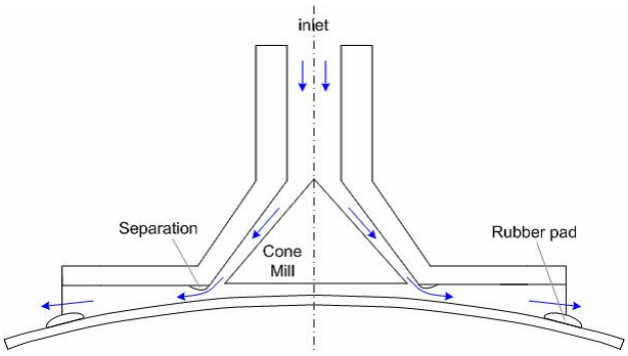

Figure A.2: A Schematic of the working of a Bernoulli thin wafer handler.

In this figure the outflow of air, creating an under pressure, as dictated by Bernoulli's law, under the handler pad is shown. Based on the same working principle is the example of A.3.
Here a swirling outflow is used to create the under pressure under the pads of the wafer handler.

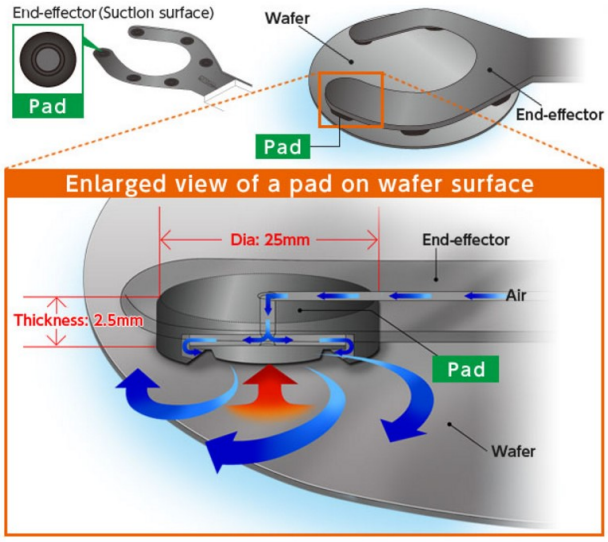

Figure A.3: A Schematic of the working of a Bernoulli thin wafer handler.

Electrostatic thin wafer handling

Below a schematic for electrostatic wafer handling is shown in A.4.

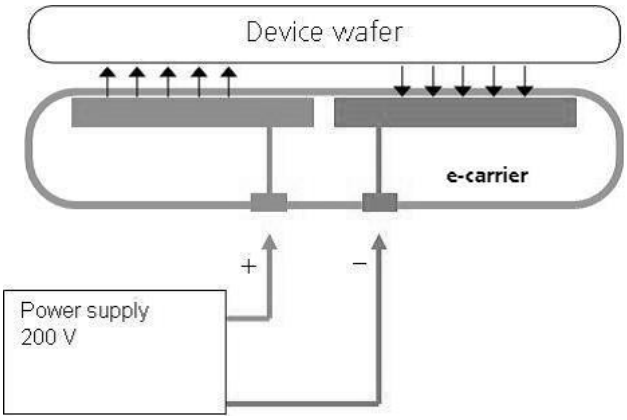

Figure A.4: A Schematic of the working of an electrostatic thin wafer handler.

The principle of electrostatic wafer handling is based on running alternating charges trough a plate, creating electrostatic forces to attract the wafer to the handler. This force can be calculated using A.1.

$$F = \frac{\epsilon A U^2}{8d^2} \tag{A.1}$$

Below an example of such a handler is shown in A.5.

This figure shows an electrostatic wafer handler made from silicium(wafer material). The reason often electrostatic carriers are made of this is because the wafer and handler then have the same properties in terms of conductivity and expansion.
An important feature of electrostatic handling is that the wafer is suspended over or under the handler without touching the handler. This is a benefit with repect to not having high stresses in

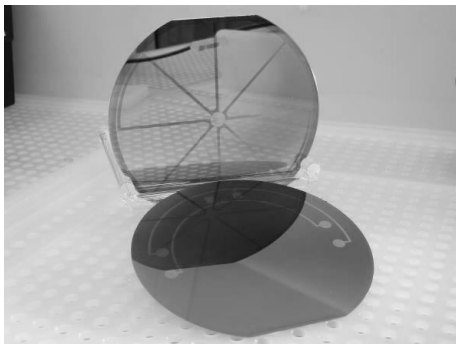

Figure A.5: An example of an electrostatic handler for thin wafer handling

contact points, since there are none. However this also means there is no frictional force holding the wafer when the handler is moving in horizontal direction, which could cause the handler to loose the wafer during handling.

Mechanical thin wafer handling

Shown in A.6 is an example of a mechanical thin wafer handler.

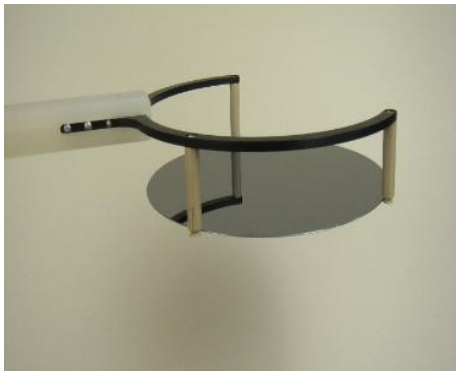

Figure A.6: An example of a gravity/friction force based handler for thin wafer handling

Mechanical thin wafer handling is based on the force of gravity and friction forces between the wafer and the handler in the contact points. As visible in this example picture, there are few contact points for mechanical handlers, which are also small, resulting in a high force on a small surface of wafer material leading to high stresses in the wafer.

Temporary bonding for thin wafer handling

Temporary bonding for thin wafer handlers is a chemical process in which extra material is bonded to the wafer to have more thickness for processing the wafer in the back end process. An overview of this process is shown in A.7.

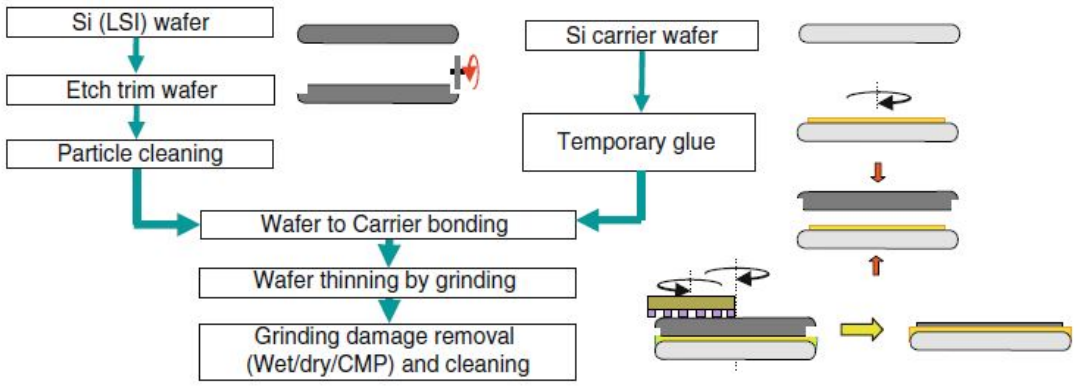

Figure A.7: An example of a possible temporary bonding process

This handling method adds extra process steps to the process, however the handling principle used could be the same as for standard thickness wafers. One other disadvantage of this handling method is the fact that the substrate carrier needs to be debonded when the wafer is thinned, with several processes extering extensive force on the wafer.

Overview

An overview of the thin wafer categories and the accompanying handling principles possible for these categories is shown in A.8.

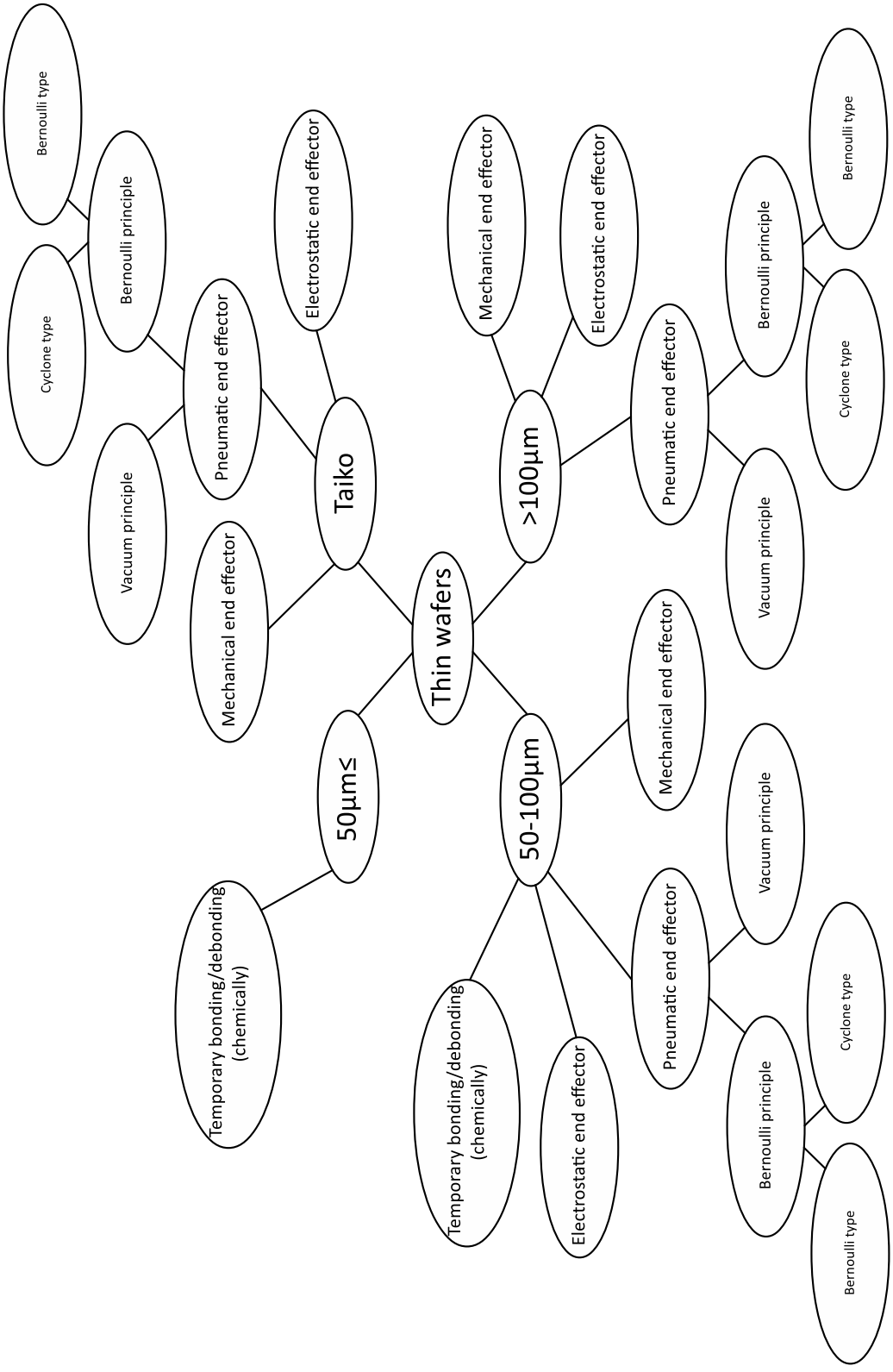

Figure A.8: An overview of the handling principles per thin wafer category

Appendix B - Burl to wafer stress, deflection and hertze contact calculations

Piece of wafer determination for euler beam analysis

$$A_{bb} = (B_p - D_b)D_b \tag{B.1}$$

$$q_{_{Fz}} = \frac{F_z}{A_{bb}} D_b \tag{B.2}$$

$$q_{_{Pv}} = P_v D_b \tag{B.3}$$

$$q = q_{_{Fz}} + q_{_{Pv}} \tag{B.4}$$

$$q = \left(\frac{-F_z}{A_{bb}} + P_v \right) D_b \tag{B.5}$$

$$q = \left(\frac{-F_z}{A_{bb}} + \frac{F}{A_{bb}} \right) D_b \tag{B.6}$$

$$\delta = -\frac{5}{384} \frac{ql^4}{EI} \tag{B.7}$$

Stress and deflection results euler beam analysis wafer piece

The results for the stress in the centre of the beam with a varying burl radius is shown below in figure B.1.

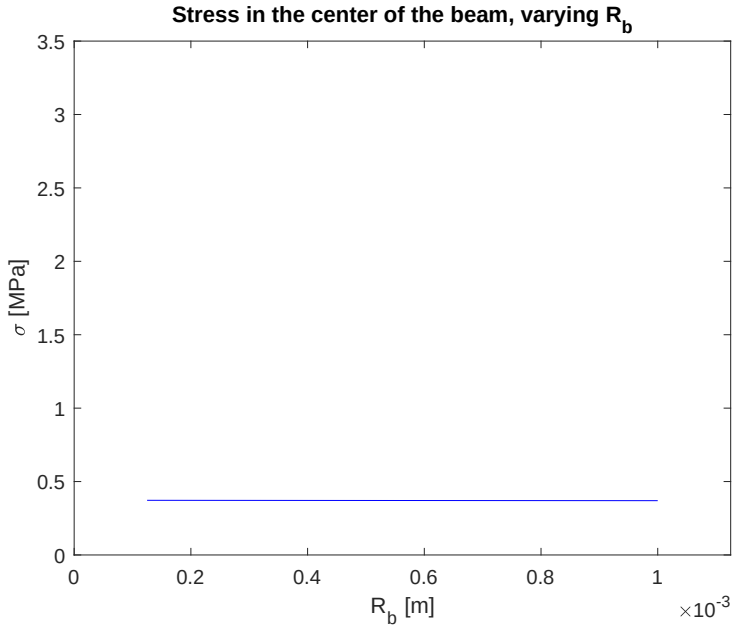

Figure B.1: Results for the stress in the middle of the beam for simulated piece of wafer for varying burl radius, burl pitch and pressure

The results for the deflection in the centre of the beam with a varying burl radius, varying burl pitch and varying pressure are shown below in figures B.2-B.4 the results are all set to the same scale on the y-axis.

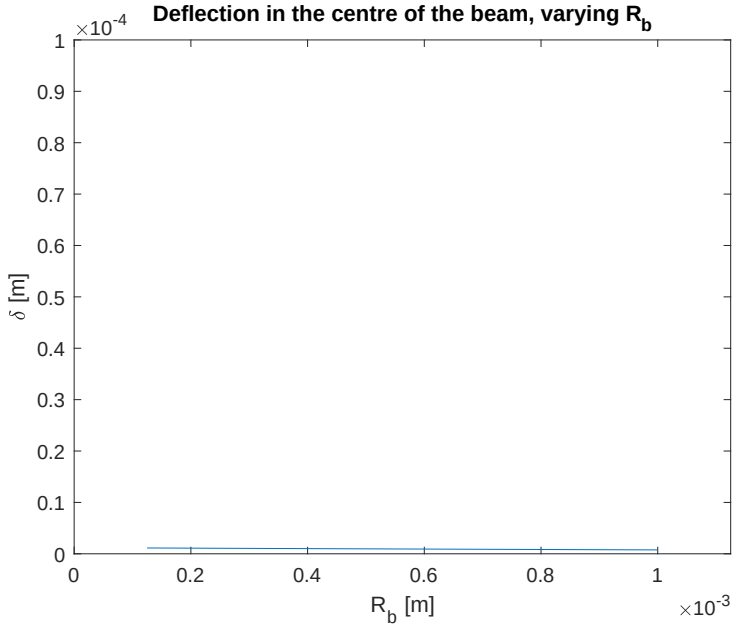

Figure B.2: Results for the deflection in the middle of the beam for simulated piece of wafer for varying burl radius, burl pitch and pressure

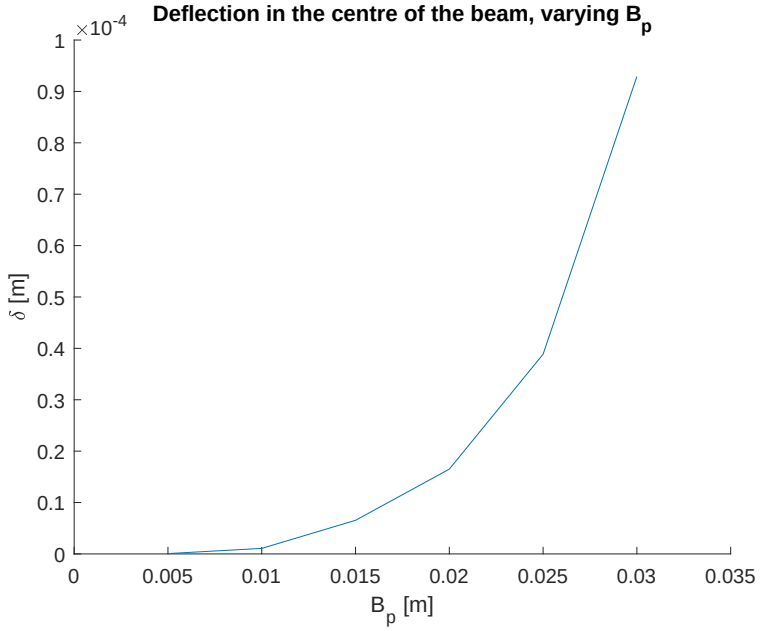

Figure B.3: Results for the deflection in the middle of the beam for simulated piece of wafer for varying burl radius, burl pitch and pressure

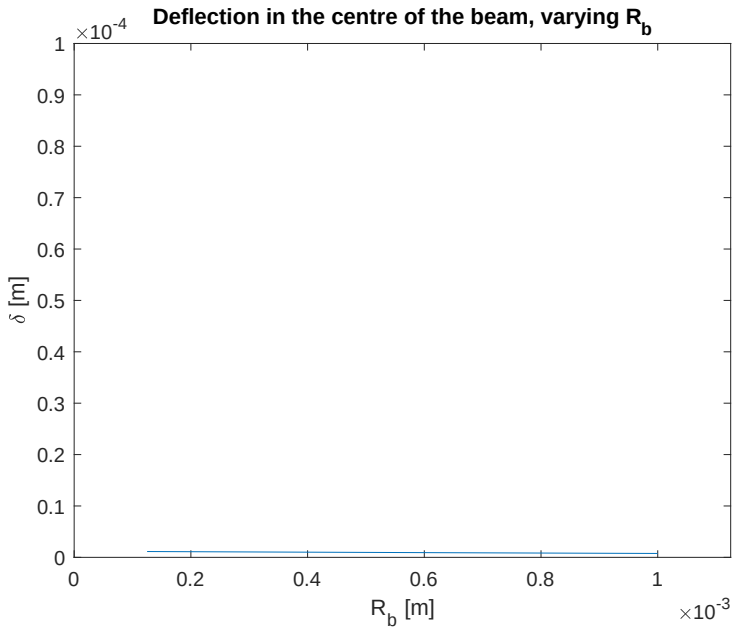

Figure B.4: Results for the deflection in the middle of the beam for simulated piece of wafer for varying burl radius, burl pitch and pressure

Appendix C

Eigen frequency analysis of the end-effector plate

Below the 1st eigenmode of the end-effector plate is shown, with $f = 181Hz$.

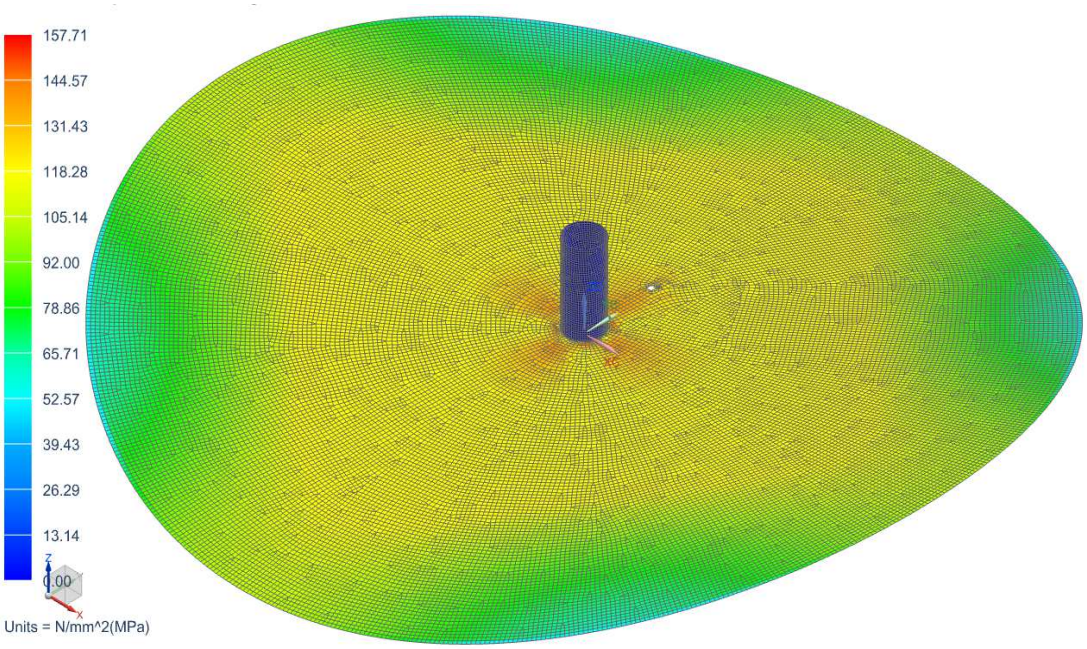

Figure C.1: Results for the eigenfrequency analysis of the end/effector plate

Appendix D

Eigenfrequency analysis graphs

Below the displacement graph for the first eigenmode, with $f = 59.0Hz$, in the case of no wafer mass added is shown in figure D.1. Figure D.2 shows the 1st eigenmode of the handler with the

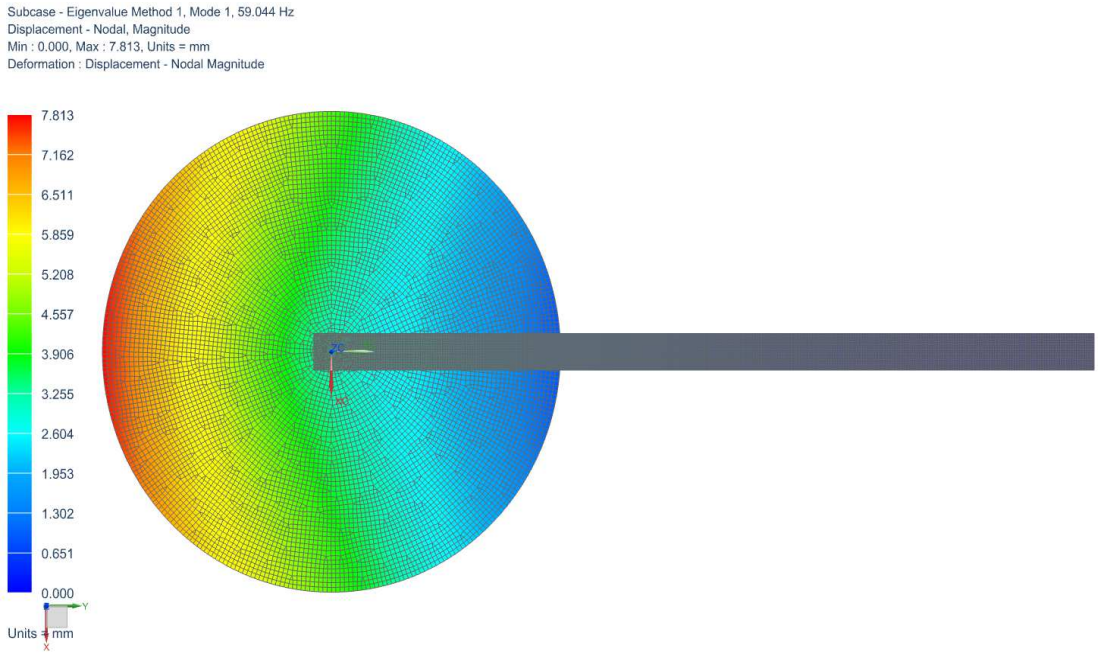

Figure D.1: Results of the eigenfrequency analysis

wafer mass added, which has an eigen frequency of $f = 56.4Hz$. Figure D.3 shows the displacement for the same eigenmode. The location with the highest stress concentration is the same as for the case without the added wafer mass.

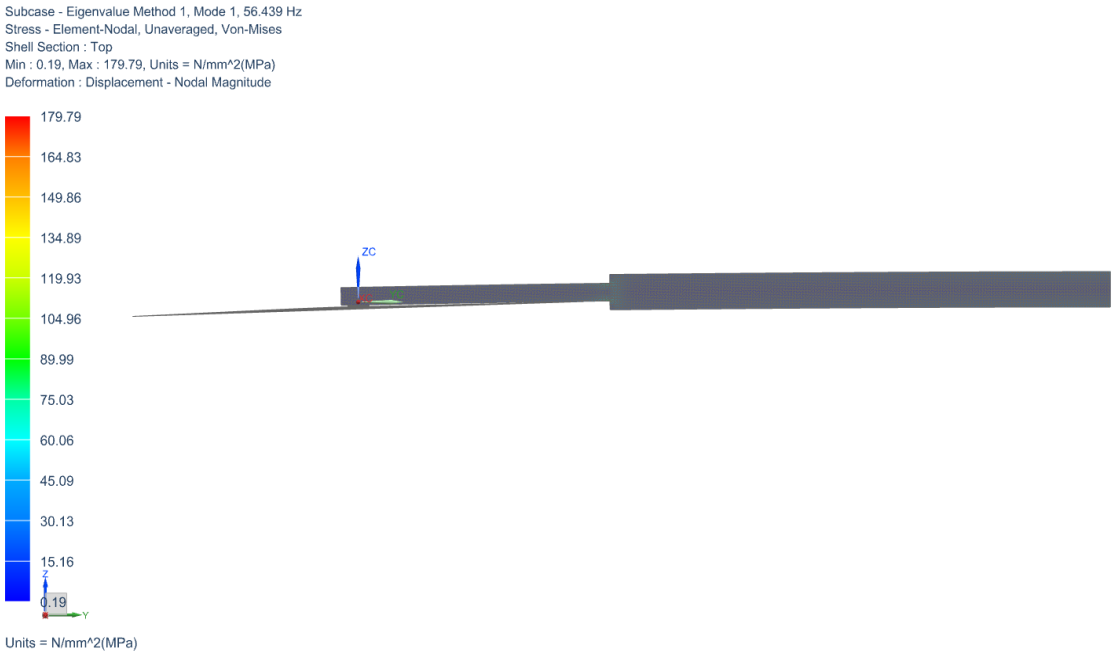

Figure D.2: Results of the eigenfrequency analysis

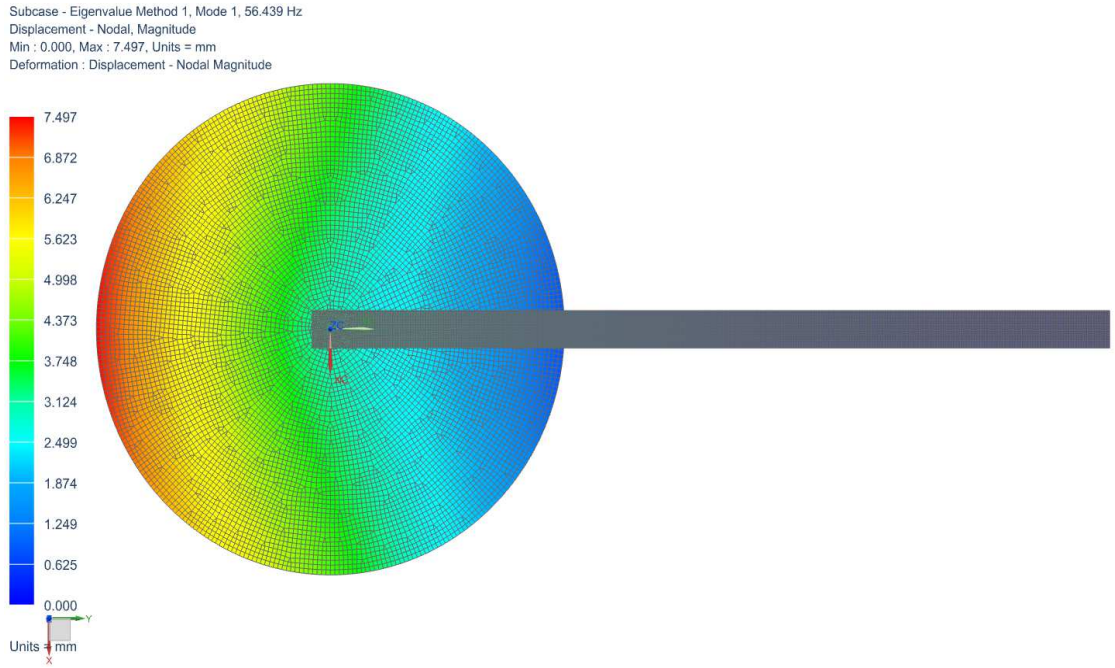

Figure D.3: Results of the eigenfrequency analysis

Appendix E

P-Q curve of the fan

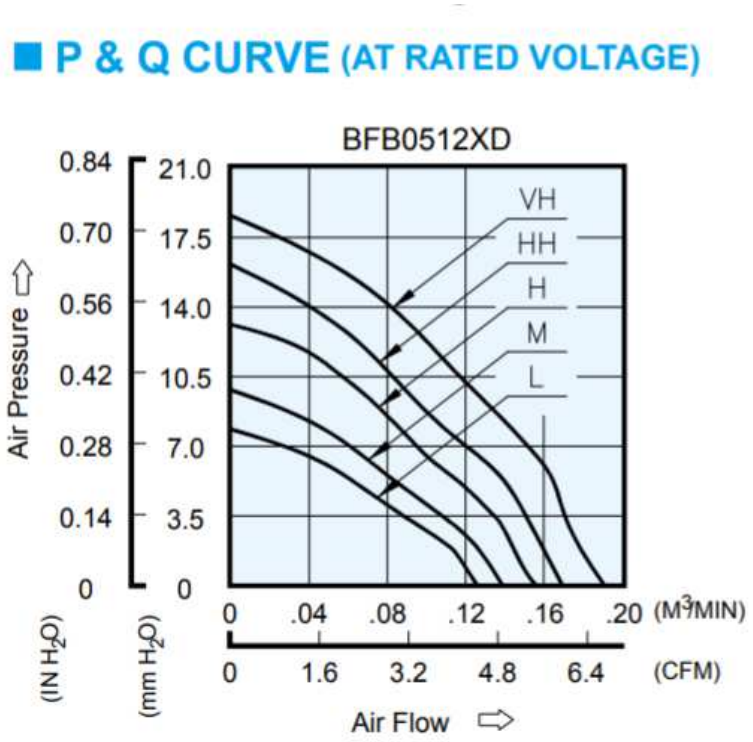

Figure E.1: PQ curve of the fan

Appendix F

In this appendix the options for the design concepts functionalities are evaluated. An overview of the functionalities, options and the considerations regarding them is shown in figure F.1 with a morphologic overview. The morphologic overview for the design concept is shown in figure F.1.

Thin wafer handler				
function	options →			
substrate interface	**flat plate** -stick together + surface area for normal force	**air bearing** + stick together - surface area for normal force	**burl layout** + stick together + surface area for normal force	
substrate interface material	**SiSiC** - contact stress - manufacturability	**Hardened steel (DLC Coated)** - contact stress -manufacturability	**PEEK** + contact stress - manufacturability	**Viton** + contact stress + manufacturability
plate material	**Steel** - density +stiffness + cost of manufacturing +/- smoothness surface waferside	**Carbon Fibre** + density +/- stiffness - cost of manufacturing + smoothness surface wafer side	**Aluminium** -density +/- stiffness + cost of manufacturing +/- smoothness surface wafer side	**Aluminumoxide** -density + stiffness - cost of manufacturing +/- smootness surface wafer side
Plate shape	**flate plate** + manufacturability +/- stiffness + waviness + flatness	**Two hollow counterparts** +/- manufacturability +/- waviness - flatness	**Hollow counterparts with baffles** - manufacturability + stiffness - waviness +/- flatness	
piping material	**PVC** +/- roughness + density - stiffness	**Glas** +roughness +/- density +stiffness + structural element - breakable	**Stainless Steel** - roughness - density + stiffness + structural element	**Aluminium** +roughness +density + stiffness + structural element
piping shape	**round** -Hydraulic diameter (based on max. height) + area moment of inertia + configurable with stock components	**ellipsoid** + Hydraulic diameter (based on max. height) +/- area moment of inertia - configurable with stock components	**square** +/-Hydraulic diameter (based on max. height) +/- area moment of inertia + configurable with stock components	**rectangular** + Hydraulic diameter (based on max. height) +/- area moment of inertia + configurable with stock components
creating under pressure	**radial fan** + low volumetric flow rate + easily tunable with pressure sensor + tunability cost effective executable	**axial fan** - high volumetric flow rate + easily tunable with pressure sensor + tunability cost effective executable	**angled fan** +/- volumetric flow rate between axial and radial + easily tunable with pressure sensor + tunability cost effective executable	**venturi tube** + flow rate dependent on reducer from pressurized air tube + easily tunable with pressure sensor - tunable at high cost

Figure F.1: Morphologic overview for the components in the design concept